The Thesis Committee for Divya Ramaswamy
Certifies that this is the approved version of the following thesis:

Effect of Surfactants on Methane Hydrate Formation and Dissociation

APPROVED BY
SUPERVISING COMMITTEE:

Supervisor:

Mukul M. Sharma

Steven L. Bryant

Effect of Surfactants on Methane Hydrate Formation and Dissociation

by

Divya Ramaswamy, B.E.

Thesis

Presented to the Faculty of the Graduate School of

The University of Texas at Austin

in Partial Fulfillment

of the Requirements

for the Degree of

Master of Science in Engineering

The University of Texas at Austin

May 2011

Dedication

To Mom and Dad

Acknowledgements

I would like to thank my graduate adviser, Dr. Mukul Sharma for his invaluable guidance, support and encouragement, which has made this thesis possible. I would also like to thank him for the patience he has shown throughout the course of my learning process. I would like to thank Dr. Steven Bryant for taking out time to read and review my work.

I am deeply grateful to Glen Baum and Gary Miscoe for their timely help and support in issues regarding all the gauges, valves and what not. I also owe thanks to Dr. Jon Holder and Harry Linnemeyer for their help in setting up the Labview program. I must thank Lionel for teaching me the tricks of making foam. I also thank Jin for her support in the form of pep talks, coffee and candies.

None of this would have been possible without my Mom, Dad and my ever-generous brother, Rajesh. I am clueless about how I should thank my friends Som, Sulaksh, Ripu, Tamanna, Sahil, Swathika, Janani, Malhar, Himanshu, Kritika, Karn for those kind and at times, not so kind words, admonishing, hugs and advice. Thanks to all of you for believing in me and supporting me in everything that I have ever attempted.

May 2011

Abstract

Kinetics of Methane Hydrate Association and Dissociation

Divya Ramaswamy, MSE

The University of Texas at Austin, 2011

Supervisor: Mukul M. Sharma

Dissociation of gas hydrates has been the primary concern of the oil and gas industry for flow assurance, mainly in an offshore environment. There is also a growing interest in the rapid formation of gas hydrates for gas storage, transport of natural gas and carbon sequestration. In this thesis, we experimentally measure the kinetics of formation and dissociation of methane hydrates and the effect of various anionic and cationic surfactants such as Sodium Dodecyl Sulfate (SDS), Cetyl Trimethylammonium Bromide (CTAB) and Alpha Olefin Sulfonate (AOS) on the association/dissociation rate constants. The importance and necessity of micelle formation in these surfactants has been studied. The effect of foam generation on the rate of formation of these hydrates has also been measured.

SDS was found to significantly decrease the induction time for hydrate formation. There was an added decrease in the induction time when a foamed mixture of water and SDS was used. On the other hand CTAB and AOS had an inhibiting effect.

The contribution of micelles towards promoting hydrate formation was demonstrated with a series of experiments using SDS. The micelles formed by these surfactants appear to serve as nucleation sites for the association of hydrates. New experimental data is presented to show that some surfactants and the use of foam can significantly increase the rate of hydrate formation. Other surfactants are shown to act as inhibitors. A new experimental setup is presented that allows us to distinguish between surfactants that act as promoters and inhibitors for hydrate formation.

Table of Contents

List of Tables

List of Figures

Chapter 1: Overview

1.1. Objective

Natural gas hydrates are a hindrance while transmitting gas at high pressures and relatively low temperatures. Undesirable formation of gas hydrates in pipelines has prompted researchers to find ways of dissociating and inhibiting their formation. While they can be a nuisance in production operations, they are also known to hold enormous potential as an energy resource and as a prospective method for transporting natural gas. In each of these applications the kinetics of hydrate formation and dissociation plays a key role. In this thesis, experiments have been performed to measure the kinetics of gas hydrate formation and dissociation and to find efficient ways of forming gas hydrates.

1.2. Overview of Chapters

The thesis is organized as follows.

Chapter 2 explains the structure, properties and applications of gas hydrates. Also included are the growth and dissociation mechanisms and a literature review of the past work on hydrates.

Chapter 3 describes the experimental set-up, including the initial set-up, the modifications made and the final experimental set-up.

Chapter 4 has a detailed description of the various steps involved in performing the hydrate formation and dissociation experiments. This includes the procedure to form hydrates using a foaming loop.

Chapter 5 presents the data and the plots for all the experiments performed.

Chapter 6 consists of the analysis of the results provided in Chapter 5 and gives reasons for various trends noticed in the experimental results.

Chapter 7 provides a summary and conclusions for the work done on methane hydrates in this thesis.

Chapter 2: Introduction

2.1. WHAT ARE GAS HYDRATES?

Water solidifying into ice is one of the best-known examples of a phase transition. This process may be altered at a suitably high pressure and a temperature that is slightly higher than the freezing point of water. The molecules then form a complex solid structure with a regular network of large and open cavities. Further cooling leads to the formation of stable ice, but in the presence of foreign molecules (such as methane), the solid structure is invaded. Methane gas is trapped within the solid complex ice structure and this compound is called methane hydrate. Although there are many other gases with suitable molecular sizes that might form hydrates (such as carbon dioxide, hydrogen sulfide and several other low carbon number hydrocarbons), methane hydrates are the most extensively found marine gas hydrates.

2.1.1. Structure

There are three main types of gas hydrates: Structure I hydrates, Structure II hydrates and Structure H hydrates. These are differentiated based on the number of water and 'guest' molecules they possess and their arrangement. Methane generally forms Structure I hydrate. This form of hydrate contains 46 water molecules surrounding 2 small cavities and 6 medium-sized cavities. The chemical formula is proposed to be $XCH_4 46H_2O$, where X can be as high as 8, but it generally takes a lower value.

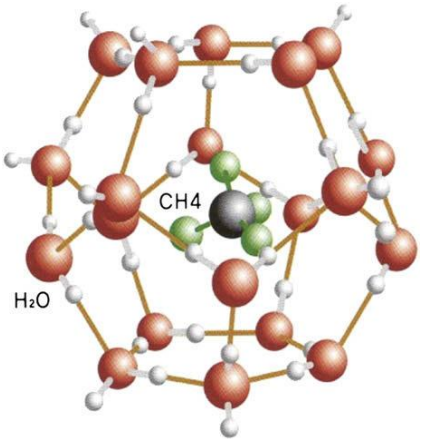

Figure 2.1: Methane Hydrate Structure (Kim et. al., 2009).

Structure II hydrate consists of 136 water molecules with 16 small and 8 large cavities. Both, structure I and structure II hydrates, are stable due to the presence of a single guest molecule within the cavities that are on average 70% occupied by the guest molecule.

The formation of structure H hydrates requires the participation of two 'guest' molecules. This unit consists of 34 water molecules with 3 small cavities, 12 larger cavities and 1 huge cavity. The larger hydrocarbon is incorporated in the biggest cavity.

According to Jeffrey and McMullan (1967), the guest molecule can be,

1. hydrophobic compounds
2. water soluble acid gases
3. water soluble polar compounds
4. water soluble ternary or quaternary alkyl ammonium salts

2.1.2. Physical Properties of Gas Hydrates

A brief summary of some of the properties of hydrates, namely their density, elasticity and electrical properties is presented below.

Density of Gas Hydrates

The density of a gas hydrate can be estimated if the parameters of a hydrate lattice, the filling ratio of cavities in the hydrate structure and the density of the former (guest) gas are known. According to Makogon (1997), the density, at equilibrium pressure and 273 K is given as follows.

Density of structure I hydrate

$$\delta^{I} = \frac{(46H_2O + 6M\alpha_1)(1/N)}{a^3} \tag{2.1}$$

Density of structure II hydrate

$$\delta^{II} = \frac{136H_2O + 8M\alpha_2)(1/N)}{a^3} \tag{2.2}$$

where,

M is the molecular weight of a hydrate;

α_1, α_2 are the filling ratios of cavities in hydrates of structures I and II, respectively;

N is Avogadro's number;

a is the hydrate unit lattice constant.

At higher pressures and temperatures the density of a hydrate can be determined with sufficient accuracy using the following equation.

$$\delta = \frac{\sum M_{hi}}{\sum V_i 18 n_i} = \frac{\sum K_i (M_{gi} + 18 n_i)}{\sum K_i V_i 18}, [g/cm^3] \tag{2.3}$$

where,

M_{hi} is the molecular weight of the hydrate of i^{th} component;

V_i is the specific volume of water in a hydrate state, g/cm^3;

K_i is the mole fraction of i^{th} hydrate former gas component with molecular weight M_{gi} in hydrate;

n is the ratio of the number of water molecules to the number of i^{th} component hydrate former gas molecules found from the following equations.

For structure I hydrate:

$$n^I = \frac{23}{\sum_{A,B,C,\kappa} \theta_1 + 3 \sum_{A,B,C,\kappa} \theta_2} \tag{2.4}$$

For structure II hydrate:

$$n^{II} = \frac{17}{2 \sum_{A,B,C,\kappa} \theta_1 + \sum_{A,B,C,\kappa} \theta_2} \tag{2.5}$$

where,

θ_1 is the filling ratio of small cavities in hydrate lattice;

θ_2 is the filling ratio of large cavities in hydrate lattice.

V_i can be calculated as

$$V_i = V_0(1 + 1.125 \times 10^{-4} \times \Delta t) \tag{2.6}$$

where,

V_0 is the specific volume of water in a hydrate state for different gases at 273.15 K and specified pressure;

Δt is temperature differential between equilibrium temperature and 273.15 K.

Electrical Properties of Hydrates

It was found (Makogon, 1974) that the presence of hydrates increases the electrical resistance of a rock. Various experiments were carried out by researchers and electrical resistance values have been measured. The following figure shows the range of electrical resistance of hydrate and hydrate saturated cores. This property has not been studied in depth. Electrical properties of hydrates are important to correctly interpret well log data when a drilled well penetrates a hydrate saturated rock.

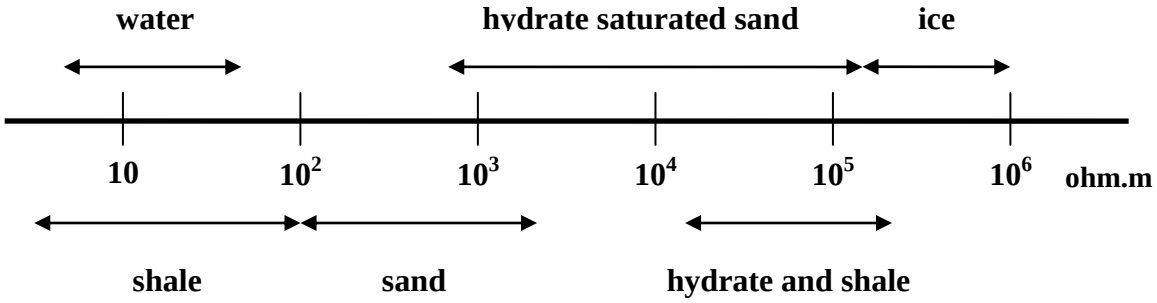

Figure 2.2: Range of electrical resistance of hydrate, sand and shale (Makogon, 1997).

2.1.3. Applications

A methane hydrate structure is a dense and compact arrangement of methane and water molecules. According to Sloan and Koh (2007), each volume of methane hydrate yields as much as 184 volumes of gas at STP. Hydrates are generally found in deep ocean environments where the temperature and pressure are appropriate for existence of stable hydrate molecules. Figure 2.3 shows the phase diagram with boundary between free methane gas and methane hydrate for a water and methane system. The presence of gas hydrates in offshore continental margins inferred from bottom-simulating reflectors has been mapped at depths below 100 m (in appropriate conditions of pressure and temperature) (Kvenvolden, 1993).

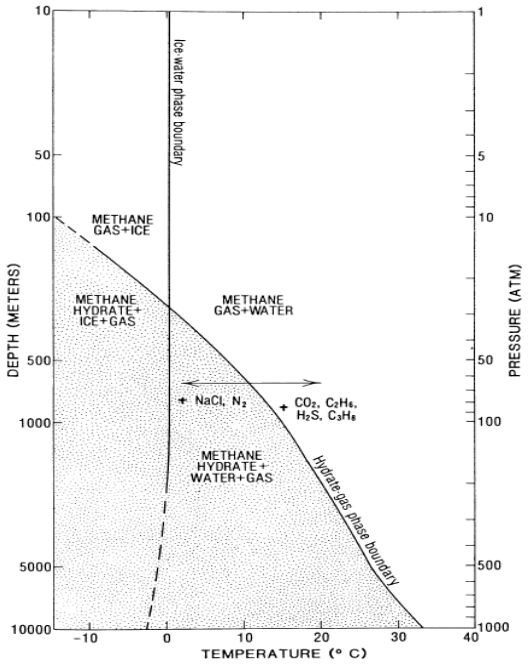

Figure 2.3: Methane hydrate stability curve (Kvenvolden, 1993).

The hydrate-gas phase boundary line separates methane hydrate from the methane gas that has dissociated from hydrate. Adding NaCl shifts this boundary to the left (in the case of sea water) whereas the presence of compounds like CO_2, H_2S etc. shifts the boundary to the right.

The energy density of methane hydrate (volume of methane at standard conditions per volume of rock) is approximately ten times that of other unconventional sources of gas, such as, coal beds, tight sands, black shales and deep aquifers (Kvenvolden, 1993). Thus, the enormous deposits of methane gas in the form of clathrate hydrate in shallow depths make it a potential energy resource.

Natural gas is conventionally transported in the form of liquefied natural gas (LNG) by cooling the gas to about -160^{o}C. Gudmundsson and Borrehaug (1996) have shown that there is a 24% cost reduction in the transportation of natural gas by ships in

the form of hydrates as compared to transport in the form of LNG. Gudmundsson and Parlaktana (1992), and Gudmundsson et al. (1994, 1995) have also demonstrated that the economics of gas storage as hydrates at higher temperatures are more favorable. However, challenges like the absence of efficient methods to form gas hydrates of high quality, optimization of the cargo system etc. need to be dealt with (Kanda, 2006). Gas hydrates are also known to have applications in water desalination and carbon sequestration.

2.2. KINETICS OF HYDRATES

2.2.1. Nucleation

Nucleation is generally defined as the onset of phase transition in a region, for example, the formation of a bubble in a liquid. Hydrate nucleation, more specifically, is the process of growth and dispersion of water and gas (CH_4 molecules in aqueous phase) clusters to achieve critical size for continued growth (Sloan and Koh, 2007). The time taken to achieve this state is called nucleation time. The process of nucleation is known to be of two kinds, namely homogeneous and heterogeneous nucleation, though homogeneous nucleation is practically very hard to achieve as it takes place in the total absence of impurities.

Yousif (1994) stated that hydrate nucleation, like any other phase transition process, is very random in nature. He explained that it is controlled by the driving force which is expressed as displacement in pressure or temperature from the corresponding values at equilibrium. Also, hydrate nucleation is dependent on the size and type of guest molecule, impurities, water history and degree of turbulence (Vysniauskas and Bishnoi, 1982).

Induction Time

Induction time or induction period is the time taken till the appearance of detectable volumes of the hydrate phase. Yousif (1994) explained induction time as time from the first contact of the hydrate forming agent (guest molecules) and water to the time of initial detection of the hydrate phase. The temperature and pressure must remain within the stable hydrate region during this period. Induction time is also known to be highly random.

2.2.2. Hydrate Growth

Hydrate growth can be carried out by either maintaining pressure and temperature constant, or keeping the volume constant. Figure 2.4 illustrates the process of hydrate growth by keeping the volume constant while gradually lowering the temperature.

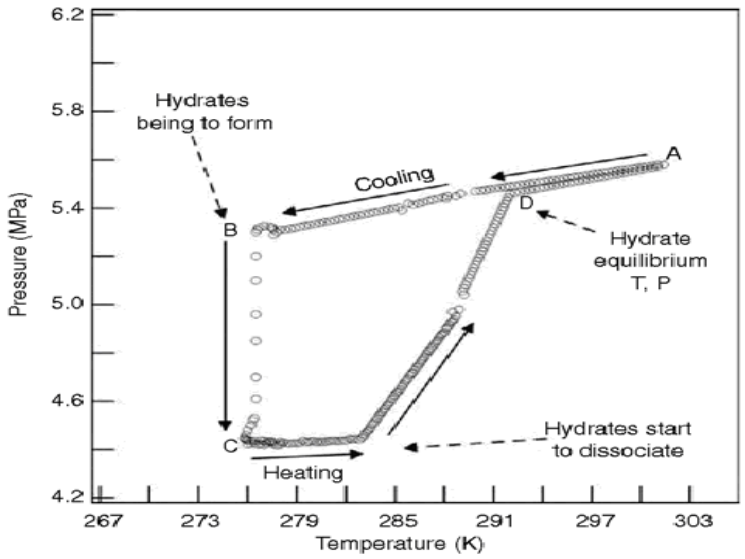

Figure 2.4: P-T trace for formation of methane hydrates (Ouar et al., 1992).

The vessel is initially pressurized with methane gas and as cooling begins, pressure decreases due to gas contraction and solubility of gas at constant volume. Due to

metastability, hydrates don't immediately form at point D. Gas solubility continues for a few more hours before hydrates finally form at point B. The period AB is referred to as the induction period. Once crystals appear at point B, there is a sudden drop in pressure due to complete hydrate formation. BC is hence the growth period. Dissociation takes place by heating up the system. Pressure increases gradually at the beginning with respect to temperature followed by a steep increase. The loop completes itself at point D where dissociation is said to be complete.

In the other method, gas is continually fed into the vessel to maintain constant pressure. Temperature is also maintained constant. Figure 2.5 shows the gas consumption versus time for hydrate formation. Region 1 is the induction time followed by the growth period where gas gets trapped in hydrate cages. As water is consumed, the slope of the gas consumption curve flattens out.

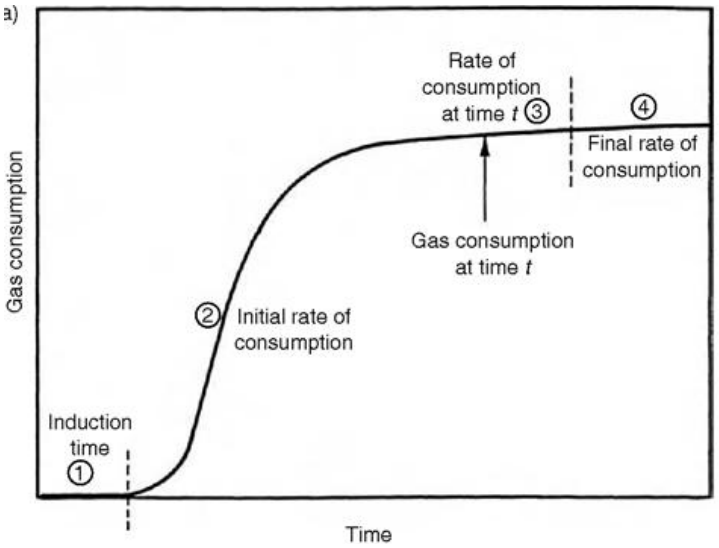

Figure 2.5: Gas consumption versus time for hydrate formation (Lederhos et al., 1996).

The method of constant volume has been used to conduct the experiments discussed in this thesis. A constant temperature is also maintained. Temperature and

pressure are recorded as nucleation and growth take place. As hydrates form, temperature spikes up and pressure drops drastically.

Crystal Growth

Gas hydrate formation has been demonstrated to be a crystallization process (Englezos et al., 1988). The process of crystallization is characterized by two distinct processes, namely nucleation and growth. The driving force of this process is the difference in the fugacity of the dissolved gas in liquid and the three phase equilibrium fugacity at the hydrate surface temperature.

$$\Delta f = f - f_{eq} \tag{2.7}$$

where,

Δf is the difference in fugacity .i.e. the driving force for hydrate crystallization

f is fugacity of the dissolved gas in liquid

eq is the three phase equilibrium fugacity at the hydrate surface temperature. This quantity represents the minimum fugacity at which hydrates can exist.

In the experiments performed, only pure methane gas has been used. The model for formation and crystal growth from pure gas has been formulated as follows (Englezos et al., 1988).

Firstly, the two step process is assumed to be

1. Diffusion of dissolved gas: The dissolved gas diffuses from the bulk of the solution to the crystal - liquid interface through the laminar layer around the particle.

2. Interface reaction: The gas molecules are adsorbed into the clustered water or water surfactant solution which is followed by the stabilization of the geometry of the structured water.

Since there is no accumulation, the rates of the above two processes are equal. Also, it is assumed that outside surface of the surrounding layer is equal to the inside surface, which is the surface of the particle. The particles are assumed to be spherical.

Following these assumptions, the rate of growth per particle is obtained as

$$\left(\frac{dn}{dt}\right)_P = K^* A_p (f - f_{eq}) \tag{2.8}$$

$$\frac{1}{K^*} = \frac{1}{k_r} + \frac{1}{k_d} \tag{2.9}$$

where,

n is moles of the gas consumed for hydrate formation

P is pressure

K^* is combined rate parameter, mole/m^2 MPa s

A_p is surface area of the particles, m^2

k_r is reaction rate constant, mole/m^2 MPa s

k_d is mass transfer coefficient around the particle, mole/m^2 MPa s

The parameter k_r accounts for the 'reaction' step, which is the adsorption of the gas molecules into the cluster-like water structure and the stabilization of the lattice. K^* is approximately equal to k_r, as it is expected that $k_d >> k_r$ (Englezos et al., 1987). It was deduced from the data and experiments that the overall gas consumption is directly proportional to the magnitude of the driving force (Δf), more than the pressure. For the

same experimental pressure and temperature, the driving force was found to decrease with increasing methane concentration.

2.2.3. Hydrate Dissociation

Similar to the growth process, the dissociation of hydrates, which is an endothermic process is also a two step process that involves the decomposition of the clathrate lattice at the surface of the particle, followed by desorption of the guest gas molecule from the surface. As decomposition progresses, the particle shrinks and the produced gas enters the bulk phase. In this case the driving force is the difference between the fugacity of the gas at the three phase equilibrium pressure and fugacity of the gas in the bulk phase.

The rate of decomposition is given by

$$-\left(\frac{dn_H}{dt}\right)_P = K_d A_p (f_{eq} - f) \tag{2.10}$$

where,

n_H is the number of moles of methane in the hydrate

P is pressure

K_d is the hydrate decomposition constant, mole/m^2 MPa s

A_p is the surface area of the particles, m^2

Memory Effect

It has been demonstrated that hydrates retain their "memory" after their formation. That is, after the hydrates dissociate, if the same solution of water or water-surfactant solution is used again, then the hydrates form faster .i.e. the nucleation time is lesser. This effect is diminished, if the system is heated to a temperature sufficiently higher than the temperature at which the hydrates dissociate (Sloan, 2007).

2.3. LITERATURE REVIEW

2.3.1. Background Information on Gas Hydrates

Sir Humphrey Davy (1811) documented natural gas hydrates for the first time. The next century saw researchers trying to find and explore the different possibilities of gas hydrate formation in terms of compounds that form hydrates, the properties and conditions of hydrate formation.

It was in the mid 1930s that Hammerschmidt (1934) discovered gas hydrates in natural gas pipelines. This discovery led to the beginning of an entirely new era of research on gas hydrates. It was in the same year that Hammerschmidt discovered thermodynamic inhibitors too. Von Stackelberg and Muller (1951) confirmed Claussen's (1951) proposal of structure II hydrate crystal structure. In 1952, the structure I hydrate was confirmed by Claussen and Polglase, Muller and von Stackelberg; and Pauling and Marsh. In the following 50 years, there have been studies and findings on the thermodynamic behavior, phase equilibria and NMR measurements of hydrates.

Once the capabilities of methane hydrate to act as a storage and transportation option for natural gas were realized, there was an array of work related to that area. It was as early as 1942 that Benesh investigated the storage and transportation of natural gas in hydrate form. In the 1990s, Gudmundsson et al. (1994, 1995) and Gudmundsson and Parlaktuna (1992) proved that the economics of gas storage in hydrates at higher temperatures are favorable. Gudmundsson and Borrehaug (1996) also stated that the transportation of natural gas by ships in the form of hydrates have better economics than their transport in liquefied form.

Hydrates are also a potential unconventional source of energy. Makogon et al. (1965) discovered massive deposits of hydrates in Siberian permafrost. Thereafter various deposits were identified in different parts of the world including Russia, USA and

India. The following three conclusions were drawn by Trehu et al. (2006) about naturally occurring hydrates.

1. Stable hydrates are generally present in water depths of 300 to 800 m.
2. Thermogenic hydrates are prevalent only at a few sites such as the Gulf of Mexico and Caspian Sea.
3. Biogenic hydrates are found in places where organic carbon accumulates rapidly, such as continental shelves and enclosed seas.

Biogenic and Thermogenic Processes

Biogenic processes occur at shallow depths and low temperatures, primarily by anaerobic decomposition of sedimentary organic matter. Biogenic gases are dry and are composed almost entirely of methane. On the other hand, thermogenic gases form at deeper depths by the thermal cracking of sedimentary organic matter and might contain wet gas components like ethane, propane or butane in addition to methane, which is the main component.

2.3.2. Previous Work on Kinetics of Methane Hydrates

Vysniauskas and Bishnoi (1982) studied the kinetics of methane hydrate formation and found that water history had an effect on the rate of formation. They also proved that stirring rate had an effect on the rate of formation, in addition to proposing a thermodynamic model. Stirring rate is directly related to interfacial area. Englezos, Bishnoi, Kalogerakis and Dholabhai (1987) proposed an intrinsic growth model which was an extension of the model for pure component hydrate formation. Englezos et al. (1988) proposed that hydrate formation is a crystallization process which involves two steps, nucleation and growth, with Δf being the driving force (Eq. 2.9).

Kalogerakis et al. (1993) tested the effects of different kinds of surfactants on hydrate formation. They concluded that surfactant concentrations near critical micelle concentration (CMC) did not affect the thermodynamics of hydrate formation, but they had an appreciable effect on the kinetics and the mass transfer coefficient. It was also shown that Sodium Dodecyl Sulfate (SDS) being an anionic surfactant had a stronger effect on the formation kinetics as compared to its cationic and non-ionic counterparts. Zhong and Rogers (2000) quantified the effect of different surfactants, and specifically their CMCs, on the rate of formation. They also performed experiments with different concentrations of SDS. Lin et al. (2004) also studied the effects of concentration of SDS on the association and dissociation of hydrates.

Sloan et al. (1998) presented the microscopic kinetics model using Raman spectroscopy and also gave an account of the macroscopic aspects of natural gas hydrate kinetic inhibition. Kashchiev and Firoozabadi (2002a, 2002b, 2003) published a series of work on quantifying microscopic level processes like crystallization, nucleation, and induction.

Sun et al. (2003) showed that the storage properties of gas hydrates can be enhanced by formation using promoters like micellar surfactant solutions. They found that SDS (anionic), Dodecyl Polysaccharide Glycoside (DPG) (non-ionic), and a mixture of SDS and DPG, had positive effects on formation rate and storage properties.

Increasing the interfacial area of contact between gas and liquid is an important factor for improving the rate of hydrate formation (Vysniauskas and Bishnoi, 1982). Stirring is one of the methods to increase interfacial area, but it is economically not viable (Zhong and Rogers, 2000). On the other hand, foaming is more efficient, both economically and experimentally. Leske et al. (2007) studied the effect of foaming, volume of foam and bubble size, and concluded that the volume of foam had a direct

relationship with the percentage of methane uptake. On the other hand, bubble size was found to have an inverse relationship with the percentage transformation of methane into hydrate. Pakulski (2007) confirmed that foaming increases the liquid - gas contact and in turn accelerates gas transport.

Chapter 3: Experimental Set-up

3.1. PRIMARY EXPERIMENTAL SET-UP

The set up primarily consists of a stainless steel hydrate cell, a refrigerated bath (Model: Neslab RTE-17) with a 50% water and 50% ethylene glycol solution, a methane gas tank, a pump, a line filter, a transducer and a thermocouple (Figure 3.1). The stainless steel high pressure variable volume cell (Figure 3.2) has an internal length of 14.96 cm, an inner diameter of 1.785 cm. and a volume of 42.25 cm^3. There are 3 sapphire windows on the cell, a large one at one end of diameter 1.785 cm and two small ones through the middle, of 1.1 cm diameter each. The transducer and thermocouple are used to measure the pressure and temperature inside the cell. The delivery of methane to the cell through tubings is controlled by a number of valves. Water or water-surfactant solution is pumped into the cell through thin stainless steel tubes and a line filter. The cell is cooled by a 0.25 inch copper tube coiled tightly around it, through which the water-ethylene glycol solution is circulated. This set-up is then insulated by using glass wool and insulation foil (Figure 3.4).

Pressure and temperature inside the cell is measured every 10 seconds as the reaction (either association or dissociation) progresses and recorded on Labview via the Data Acquisition (DAQ) board to which the transducer and the thermocouple are connected (Figure 3.6). This data is then used to analyze the pressure, temperature and time correlations.

3.2. MODIFICATIONS MADE TO THE INITIAL SET-UP

A number of modifications have been made to the primary set up. Firstly, a temperature feedback control loop has been installed. This was incorporated to ensure

that the cell is maintained at a constant temperature throughout the entire process, and the temperature of the cell is within the methane hydrate stability temperature window. The temperature of the cell is recorded continuously and when this temperature deviates from the set point, the refrigerated bath (Figure 3.3) regulates the temperature of the water-ethylene glycol solution, which in turn heats/cools the hydrate cell back to the set temperature. The feedback loop has been established by connecting the bath in the series communication mode to the computer interface using the NI Labview program.

The methane gas has also been circulated through the refrigerated bath to ensure that the gas entering the cell is not at room temperature. This has helped reduce the time taken for the refrigerator to cool the cell down after gas and water injection.

The most important addition to the set up has been the inclusion of a flow loop to form foam. The process of this flow loop is discussed in detail in the following chapter.

A schematic and the components of the set-up are shown in Figures 3.1 through 3.6.

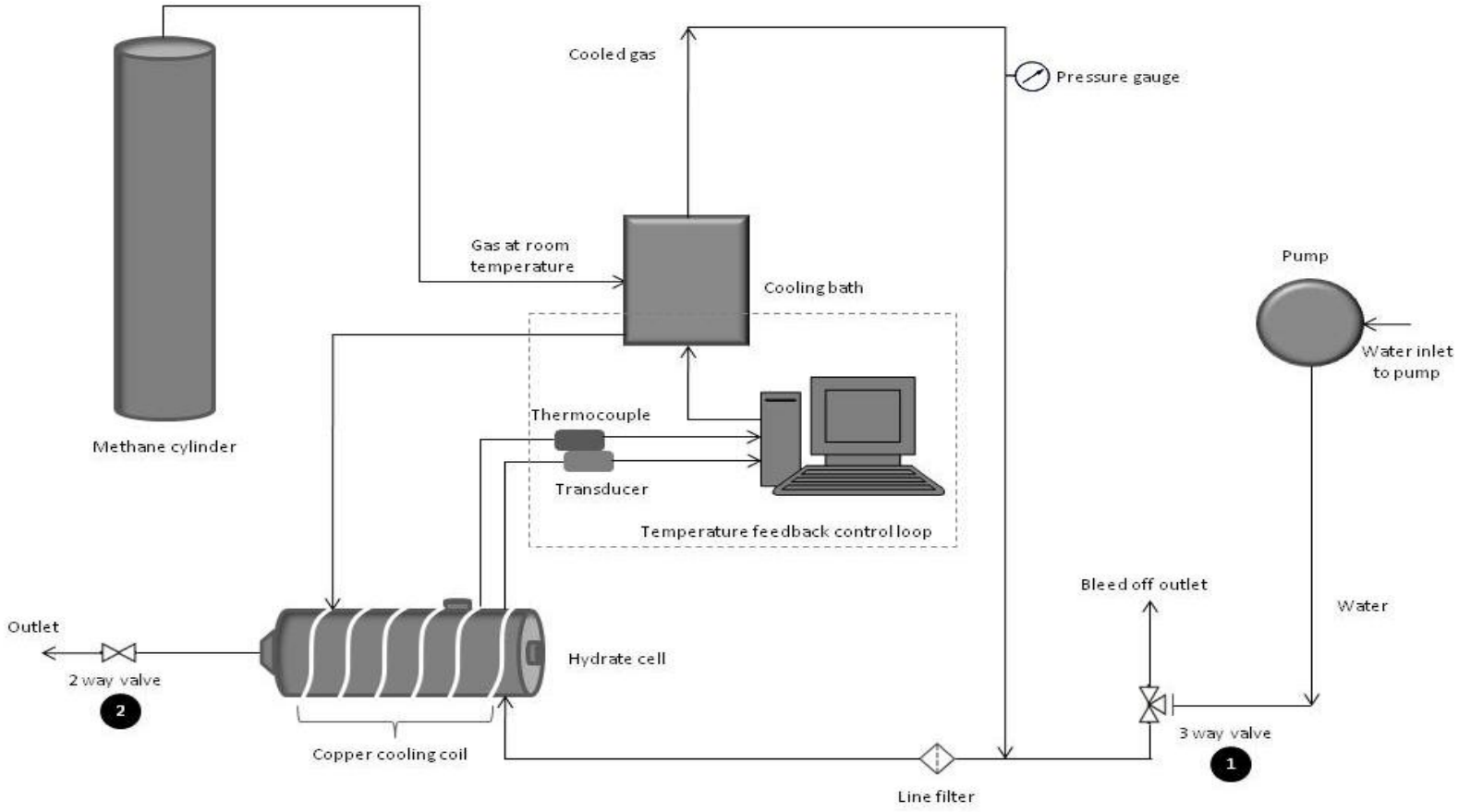

Figure 3.1: Schematic of the final set up for hydrate formation and dissociation.

Figure 3.2: Hydrate cell with cooling copper coil with glass wool and foil insulation.

Figure 3.3: Refrigerating bath with 50% ethylene glycol and 50% water solution.

Figure 3.4: Hydrate cell connected to refrigerating bath inside fume hood.

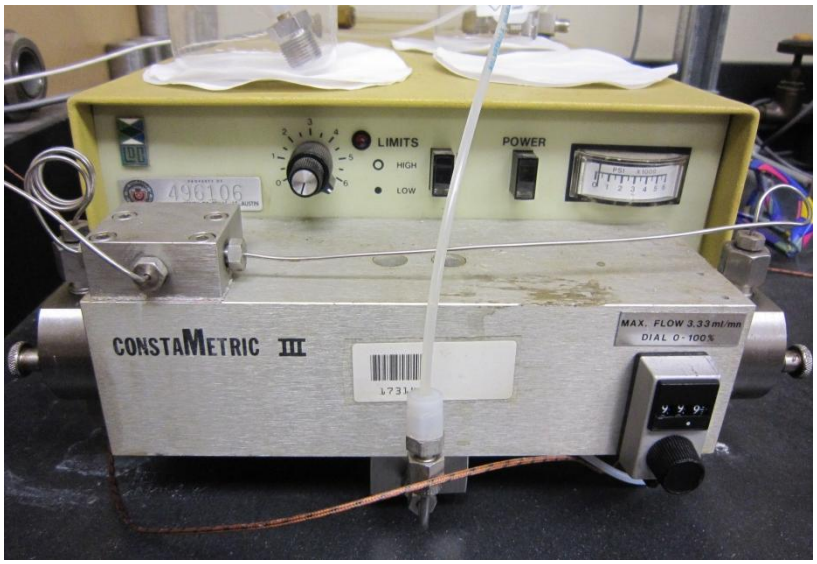

Figure 3.5: Pump through which water or water surfactant solution was pumped into the hydrate cell.

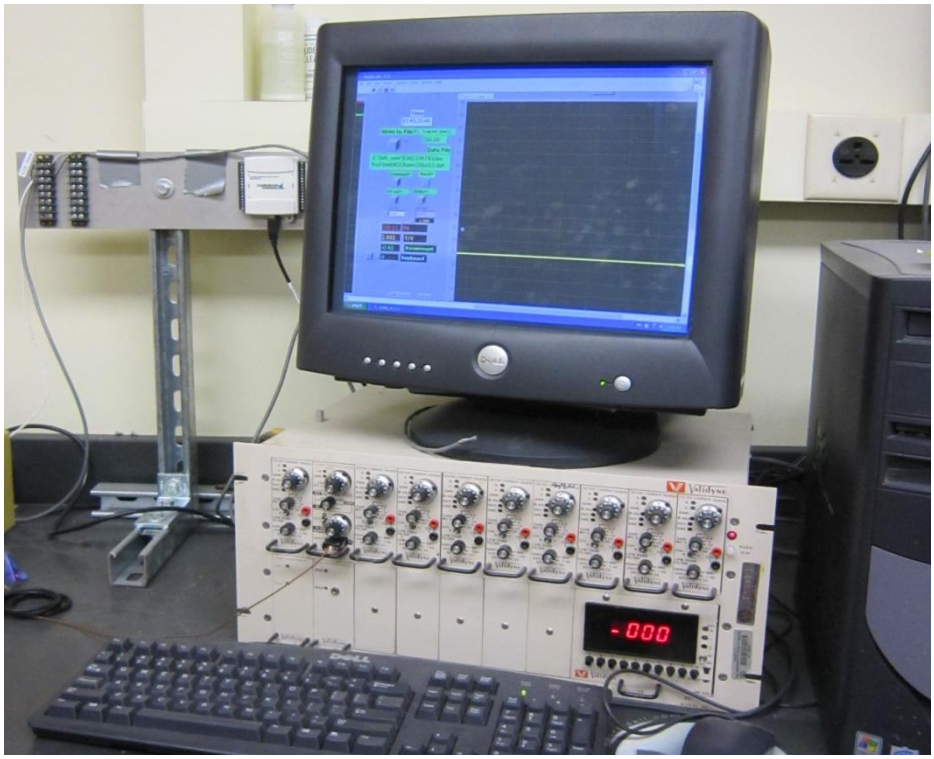

Figure 3.6: Computer with NI Labview connected to the pressure transducer and thermocouple through a DAQ board.

3.3. FINAL EXPERIMENTAL SET-UP

3.3.1. Inclusion of flow loop for formation of foam

The final experimental set up includes a flow loop (Figures 3.7 and 3.11) with a liquid and gas inlet for making foam. Water-surfactant solution is pumped into the loop, following which gas is injected. After a certain amount of gas is injected, the solution is circulated through the loop with the help of a circulating pump (Figure 3.10). Gas is injected periodically and the cycle continues until the required quality of foam (Eq. 3.1) is obtained, which can be determined from the reading on the mass flowmeter (Figure 3.9) that is connected to the loop.

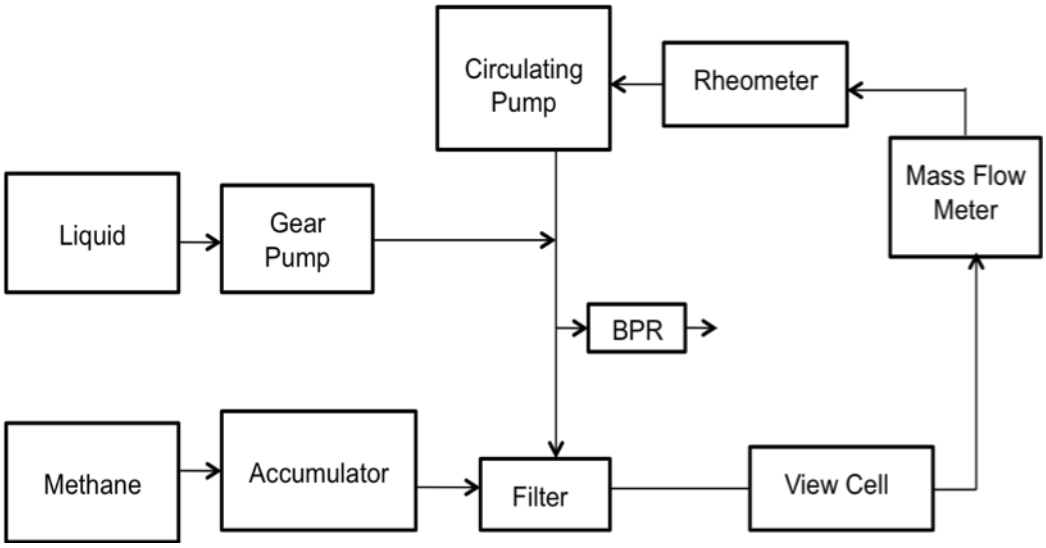

Figure 3.7: Block diagram for foam producing flow loop.

Figure 3.8: Pump through which liquid phase is pumped into the foam flow loop.

Figure 3.9: Mass flow meter used to assess density, rheology of the foam inside the loop.

Figure 3.10: Circulating pump connected to flow loop.

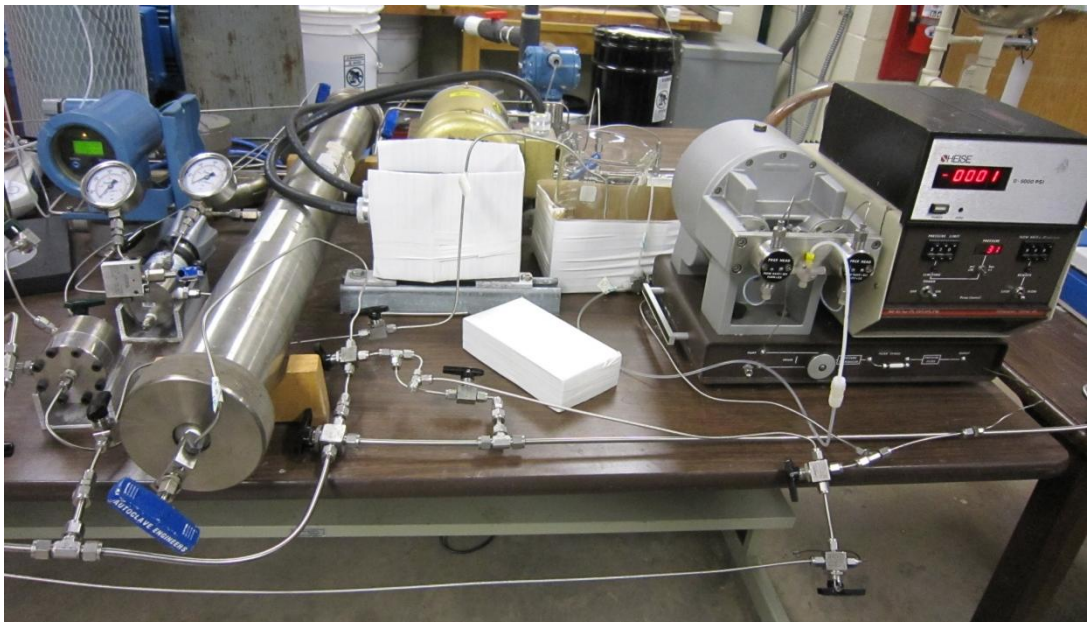

Figure 3.11: The entire foam formation flow loop.

After the required quality of foam is obtained, it is transferred into an accumulator at the same pressure. The foam is then transferred into the hydrate cell by pressurizing the hydrate cell to the same pressure as the foam in the accumulator and slowly feeding in the foam to the cell by releasing pressure from the other end of the cell. A piston might also be used for this purpose.

3.3.2. What is foam?

Foam is a mixture of a continuous liquid phase and a discontinuous gas phase. Typical foams used in lab scale are N_2-water and CO_2-water, with some additives such as foamers, stabilizers, polymers, etc. For the gas hydrate experiments, foam of CH_4 gas and water-surfactant solution has been used.

Foams are classified according to their quality or volume fraction of the gas phase. Quality of foam is given as

$$\tau = \frac{V_{gas}}{V_{gas} + V_{liquid}} \tag{3.1}$$

3.3.3. Types of surfactants

Surfactants are organic compounds that lower the surface tension of a liquid by adsorbing at the interface between two fluids. They are amphiphilic i.e. they have both hydrophobic and hydrophilic groups. Hence they have a water insoluble and a water soluble component and can be symbolized as having a polar (hydrophilic) 'head' and a non-polar (hydrophobic) 'tail'.

The most common classification of surfactants is based on their dissociation in water. They are classified as follows.

Anionic Surfactant - In these compounds, the hydrophilic head is negatively charged. The most widely used anionic surfactants are carboxylates, sulfates, sulfonates and phosphates.

Cationic Surfactants - In these compounds, the hydrophilic head is positively charged. Two common types of cationic surfactants are long chain amines and quaternary amine salts, though their usage is less when compared to anionic and non ionic surfactants.

Non-ionic Surfactants - In these surfactants, the hydrophilic head is polar, but not fully charged. Of the several types of nonionic surfactants, the polyoxyethylenated nonionic surfactants are the most common.

Of the above mentioned surfactants, Sodium Dodecyl Sulfate (SDS), Alpha Olefin Sulfonate (AOS) and Cetyl Trimethylammonium Bromide (CTAB) were used for the experiments. The first two are anionic surfactants and the last one is a cationic surfactant.

Chapter 4: Experimental Procedure

4.1. PROCEDURE FOR EXPERIMENT WITH ONLY THE HYDRATE CELL

The general procedure for all the experiments is outlined. The following procedure has been used to perform experiments without the foam from the flow loop. The procedure including the flow loop is outlined later.

1. The cell and the tubings are cleaned by flowing water for a period of 20 minutes.
2. As the water passes through the set up, the equipment is checked for leaks and joints are tightened as necessary. Also, the pipelines are checked for blockages before starting the experiment.
3. The cell is then purged with methane for short intervals of time to expel any trapped air.
4. The pipes are then purged with the liquid solution that is to be used in the experiment.
5. Once these preliminary steps have been carried out, the cooling bath is switched on and set at a temperature of 2.5 ℃, which lies in the methane stability window. Once the temperature of the cell stabilizes, if foam is desired, water is injected first else gas is injected first.
6. If foaming method is desired, the cell is initially charged to 200 psi with methane. Next, water or water-surfactant solution is passed and the amount of liquid injected is calculated from the change in this pressure. Following this, the cell is charged again to the final pressure of approximately 1200 psi with more gas.

7. The amount of liquid to be injected is calculated using the Boyle's law equation, $P_1V_1 = P_2V_2$ such that the water to gas ratio required to form gas hydrates is attained. In these set of experiments, structure I hydrates are formed which have a water to gas ratio of 1:5.75.
8. The cooling loop is open at all times to ensure that the temperature of the cell after injection of gas and liquid is maintained at the set temperature.
9. If non-foaming method is desired, the steps are reversed. Gas is first fully injected to pressure P_1 in the 'gas first' calculations shown in Figure 4.1, followed by water till final pressure P_2 is reached.
10. The NI Labview recorder is switched on and the data is written to a file.
11. After this, the sample is left undisturbed till hydrates form which can be determined by a sudden drop in pressure and can be confirmed through the view port.
12. Once the gas hydrates form, dissociation is carried out by raising the bath temperature to about 12 ℃. The cell is left undisturbed till dissociation is complete.
13. Valve 2 is used to depressurize the cell. Once all the pressure is released, the cell is opened up and cleaned.

4.1.1. Cleaning the Cell

Before starting an experiment, any leftover gas or liquid from previously conducted experiments needs to be cleaned. Deionized (DI) water is passed through the whole set-up, by opening valves 1 and 2. Once the cell and tubings are cleaned, air is purged through. While passing water, the set-up also needs to be checked for leaks. Once these precautions have been taken, gas is purged through the set-up in quick successions.

The cell is then cleaned using a vacuum pump. This ensures that there are no air pockets present before the start of the experiment.

4.1.2. Temperature Stabilization

Methane hydrate, as already discussed, forms within a certain P-T window. Maintaining the pressure is fairly easy when compared to stabilizing the temperature. Since the association reaction is exothermic, the temperature increases during the reaction. Hence, to stabilize the temperature, a temperature feedback loop has been installed which has been described earlier.

4.1.3. Loading the Cell

Depending on whether foam is required, gas or liquid is injected. In case foaming method is to be carried out, liquid is injected after a little gas. For example, initially 200 psi (P_1) of methane is loaded into the cell followed by the required amount (13 ml) of liquid till pressure P_2 is attained (Figure 4.1). The cell is charged to the final pressure of 1200 psi with methane. Both gas and liquid pass through the line filter to form foam. Note that, the foam formed by this method is not of very good quality. Experiments conducted with good quality foams will be discussed later in this chapter. For non-foaming method, gas is first fully injected to pressure P_1 in the 'gas first' calculations shown in Figure 4.1, followed by water till final pressure P_2 is reached.

Once gas and liquid are loaded in to the cell, the equipment is left undisturbed till hydrates are formed which can be determined by a significant drop in pressure. In addition to this, hydrates can also be visually confirmed through the view cell.

2							
3	**Water first:**						Input
4							Calculated
5	P1	=	200	psi			Fixed
6	V1	=	42.25	ml			
7	Amt. water	=	13	ml			
8	V2	=	29.25	ml			
9	P2	=	295.4222	psi			
10							
11	**Gas first:**						
12							
13	V1	=	42.25	ml			
14	P2	=	1200	psi			
15	Amt. water	=	13	ml			
16	V2	=	29.25	ml			
17	P1	=	826.2462	psi			
18							
19							

Figure 4.1: Pressure volume input calculations.

4.1.4. Dissociation of hydrates

Dissociation of hydrates is carried out by increasing the bath temperature. As the stability of the hydrates depends on temperature and pressure, when the temperature is increased to above the P-T window, dissociation of hydrates starts taking place. The temperature is increased to 12 ℃ and the equipment is left undisturbed. As the temperature increases, the pressure increases due to release of gas from the hydrate crystals (change of solid-gas phase to liquid-gas phase). After a certain amount of time, the pressure will gradually stabilize when it can be assumed that the dissociation is complete.

4.1.5. Extraction of hydrates

Hydrates were extracted after a few experiments to visually confirm their presence. Once the hydrates form, and the pressure stabilizes after the drop, valve 2 is opened to slowly release pressure. Once a considerable amount of pressure has been released and it reaches a safe value of about 300 psi, the lid at the back of the cell is

slowly unscrewed. Note that the release of pressure might lead to disintegration of hydrates. Once the lid is opened, due to higher pressure inside the cell, the hydrate mass is pushed to the mouth of the cell. It is removed using tongs and flammability test is carried out on it.

4.1.6. Pressure and Temperature Recording

Pressure and temperature in the cell are recorded from the beginning of the experiment. The recorded data is used to determine the kinetics of formation and dissociation from P-T plots. Using these, the reactions can be compared for different surfactants and different concentrations of the same surfactant.

4.2. PROCEDURE FOR HYDRATE FORMATION USING FOAM

The procedure for hydrate formation and dissociation using foam is very similar to the one explained above, the difference being the formation of foam using the flow loop which is then transferred into the cell. The next two sections explain in detail, the flow loop set up and the process of foam formation, followed by the method of transferring the foam into the hydrate cell.

4.2.1. Flow loop set up and formation of foam

A new laboratory setup designed and built for measuring the leak-off rates of both liquid and gas phases under dynamic fluid-loss conditions has been used to produce foam of required quality. It consists of a 850-cc closed-loop system where the fluid is prepared and circulated. Gas and liquid are loaded separately to the loop through the use of reducing regulators. The liquid phase (water with surfactant) is added to the loop with a high-pressure metering pump to the required pressure. The gas phase (methane) is added to the loop through a reducing regulator connected to a 3 liter accumulator previously loaded with gaseous methane. The closed-loop contains an in-line screen (0.5 micron

mesh size), which plays the role of foam generator, a high flow-rate circulating gear pump and a high-accuracy mass flowmeter. Also, a differential pressure transducer and a viewing cell are used to control the foam stability and its rheology. The solution is circulated to guarantee its homogeneity throughout the loop. Once constant fluid temperature, density, viscosity and flow rate have been attained, the foam is diverted into a 1 liter accumulator.

4.2.2. Transferring foam into the hydrate cell

After the foam is transferred into the 1 liter accumulator, it is disconnected from the foam flow loop and connected to the hydrate cell. The cell is loaded with the foam by one of the two methods.

1. The hydrate cell is first evacuated using a vacuum pump and then the valve connecting the accumulator and the cell is opened. Due to large pressure difference, the foam automatically transfers from the accumulator to the hydrate cell.
2. The hydrate cell is first pressurized to the pressure equal to the one in the accumulator. Then the outlet valve on the cell is slowly opened when simultaneously the valve connecting the accumulator and the cell is also opened. Now the foam displaces the gas already present in the cell. Once foam is seen at the outlet of the cell, the valves are closed.

Chapter 5: Results

As mentioned earlier, pressure and temperature are recorded at time intervals of 10 seconds using NI Labview. Different plots and calculations carried out to determine the kinetics of hydrate formation are explained in this section. The hydrate formed during one of the experiments is shown in figures 5.1 and 5.2. The texture and form of the hydrates were consistent in all the experiments performed.

Figure 5.1: Cylindrical form (slightly hollow) of the hydrate formed and extracted from the cell.

Figure 5.2: Hydrates after dissociation due to exposure to room temperature and atmospheric pressure.

5.2. FORMULAE AND CALCULATIONS

The following reaction is assumed and kinetic calculations are carried out accordingly.

Methane + Water → Hydrate

Here, the water may be DI water or a DI water-surfactant solution. Note that the effect of surfactant concentration is not taken into account in these calculations as very low concentrations have been used. A typical example of the variation of pressure and temperature with time in a hydrate formation experiment is shown in figures 5.3 and 5.4. This plot is for the case with foam, above CMC of SDS. These plots are analyzed to obtain the rate constant for hydrate formation reaction.

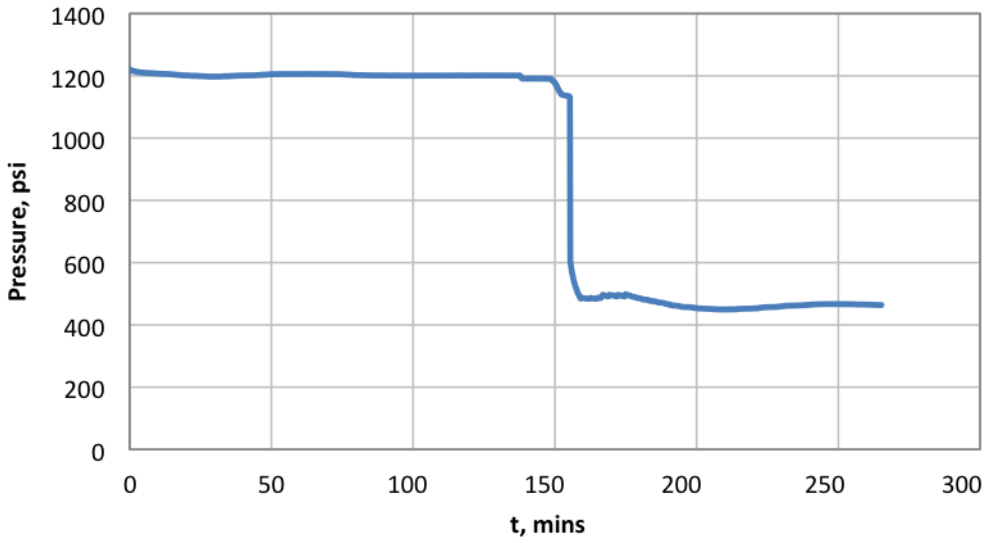

Figure 5.3: Pressure vs time for association of hydrates above CMC, with foam.

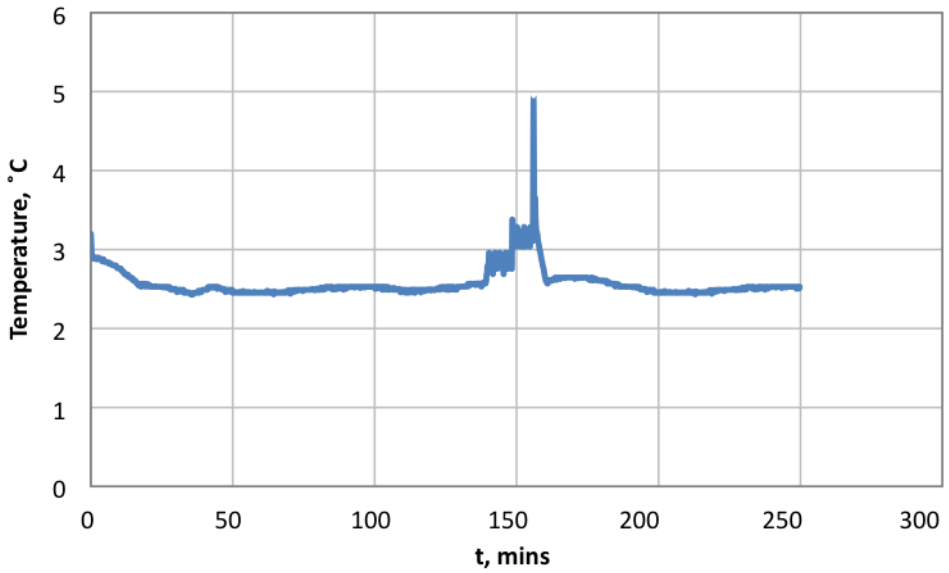

Figure 5.4: Temperature vs time for association of hydrates above CMC, with foam.

If the initial number of moles of gas is assumed to be $N_{G0,}$ the final number of moles of gas is $N_{G0}(1 - X)$, where X is the conversion, then, from the ideal gas law, pressure is given as

$$P = \frac{NRT}{V} = \frac{N_{G0}(1-X)RT}{V} \tag{5.1}$$

where,

N is the number of moles of gas

R is the universal gas constant

T is the temperature

V is the volume occupied by gas in the cell

X is the fraction (moles) of gas converted to hydrate

The volume occupied by gas changes in the constant volume cell with the reaction because water (density = 1.00 g/cm^3) is consumed and hydrate is formed. The density of

structure I methane hydrate is 0.94 g/cm^3 (Sloan and Koh, 2007). Due to the small difference in the densities, this change in gas volume has been neglected.

From Eq. 5.1,

$$P = P_0(1 - X) \tag{5.2}$$

$$X = 1 - \frac{P}{P_0} \tag{5.3}$$

In this calculation, conversion and rate have been calculated for every time step (Δt) i.e. instantaneous conversion and instantaneous rate have been calculated.

$$X(@t) = 1 - \frac{P_t}{P_{t-\Delta t}} \tag{5.4}$$

The rate is defined as the change in concentration with time.

$$r = -\frac{1}{V}\frac{dN_G}{dt} \tag{5.5}$$

In terms of hydrate formation, rate is given as

$$r = \frac{1}{V}\frac{dN_{hydrate}}{dt} \tag{5.6}$$

Eq. 5.5 can be written as

$$r = -\frac{1}{V}\frac{d[N_{G0}(1 - X)]}{dt} \tag{5.7}$$

Therefore,

$$r = -\frac{1}{V}\frac{dN_G}{dt} = \frac{1}{V}\frac{dN_{hydrate}}{dt} = \frac{N_{G0}}{V}\frac{dX}{dt} \tag{5.8}$$

From Eqs. 5.3 and 5.8,

$$r = -\frac{1}{V}\left(\frac{N_{G0}}{P_0}\right)\frac{dP}{dt} \tag{5.9}$$

In the above equation, the pressure gradient, $\frac{dP}{dt}$ is calculated as

$$\frac{dP}{dt} = \frac{P_{t+\Delta t} - P_t}{\Delta t} \tag{5.10}$$

Hence, the instantaneous rate of hydrate formation (Eq. 5.9) is calculated numerically at every time step using the change in pressure with time. Note that this is an instantaneous rate of hydrate formation that changes with time as hydrate is formed and gas is consumed.

For a rate limited reaction, the expression for the rate of hydrate formation reaction is given as,

$$r = k\left[concentration\,of\ reactant\right]^a \tag{5.11}$$

where,

$$concentration\,of\ reactant = \frac{N_{G0}(1-X)}{V} \tag{5.12}$$

Next, Eq. 5.11 was plotted graphically using the array of rate values obtained from Eq. 5.9 against the concentration of the reactant (Eq. 5.12). For a typical case, the plot obtained is shown in Fig. 5.5. From the plot, it is clearly seen that the reaction rate is not a function of the methane concentration. It can be concluded that the rate of hydrate formation is not kinetically controlled, instead the reaction is diffusion controlled. This idea is explored in detail below.

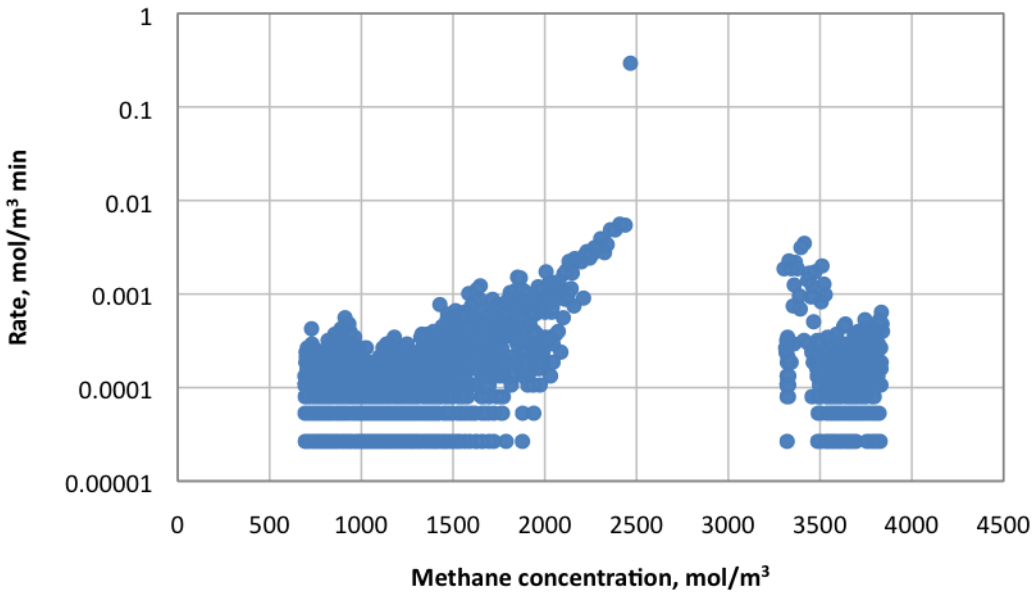

Figure 5.5: Rate vs concentration of reactant for the case with foam, above CMC of SDS

The steps visualized during the formation of a methane hydrate crystal are

Step 1: Diffusion of gaseous reactant (methane) through the film surrounding the particle to the surface of the solid (hydrate).

Step 2: Penetration and diffusion of the gas to the reaction surface.

Step 3: Chemical reaction of the gaseous reactant with the solid.

These steps occur successively for the reaction to take place and hence they can be considered as resistances in series. Due to this, whenever one of the steps offers major resistance, the step may be considered as the rate-controlling step (Levenspiel, 1998).

In this case, we assume the chemical reaction to be elementary and the diffusion of gas to the solid to be the rate-controlling step. Following this assumption, it can be safely stated that the concentration of the gaseous reactant has almost no effect and is constant. Hence, considering the growth of the surface of the solid and deriving the kinetics of the entire reaction based solely on it, we get,

$$\frac{1}{S}\frac{dN_{hydrate}}{dt} = k\left[CH_4\right] \tag{5.13}$$

where,

S is the surface area of the particle.

If in Eq. 5.13, the concentration of the gaseous reactant is assumed to be constant, then the rate of hydrate formation will be proportional to the surface area of the hydrate formed.

$$Moles\ of\ hydrate\ formed \propto S^a \tag{5.14}$$

In the above equation, *a* can be called the surface area exponent.

The amount of hydrate formed is proportional to the amount of gaseous reactant consumed.

To test this hypothesis, rate was plotted against the concentration of gas consumed (which is proportional to concentration of hydrate formed, which in turn is proportional to the surface area).

$$r = k[concentration\ of\ hydrate\ formed]^a \tag{5.15}$$

Therefore,

$$r = k\left(\frac{N_{G0}X}{V}\right)^a \tag{5.16}$$

where,

$\frac{N_{G0}X}{V}$ is the number of moles of methane consumed to be converted into hydrate.

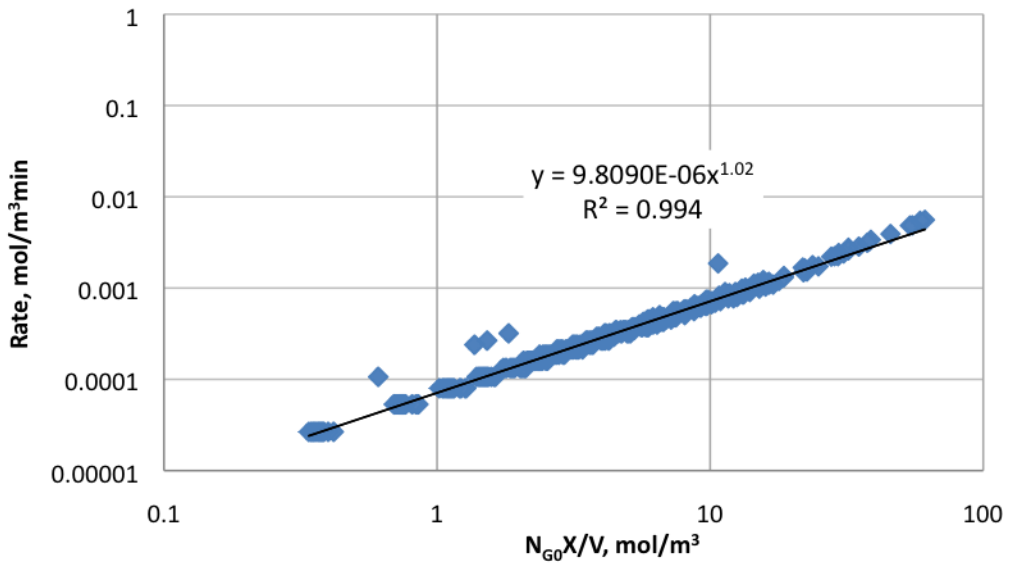

Figure 5.6: Rate vs concentration of gas consumed for the case with foam, above CMC of SDS

Figure 5.6 shows the power law relation between the rate of hydrate formation and the concentration of gas consumed. This clearly implies the relation between rate and the surface area of the hydrate formed. As more gas is converted to hydrate, the surface area increases, in turn increasing the rate of the reaction.

The values of rate constant (k) and surface area exponent (a) can be obtained from the slope and intercept of a log-log plot of rate of hydrate formation versus concentration of gas consumed.

5.3. Formation Kinetics with Surfactants

Various experiments were carried out using different surfactants, with surfactant concentrations above and below critical micelle concentration (CMC), with and without foam, and also using the external foaming loop.

5.3.1. Experiment with Deionized Water

Two experiments were conducted using deionized water as the liquid phase. The induction times for the two experiments were 6 days and 5 days respectively. Since the time taken for this case is two orders of magnitude more than the surfactant cases, the kinetics were not assessed.

5.3.2. Sodium Dodecyl Sulfate (SDS)

The following trials were carried out using SDS.

1. Without foam
    - Below CMC
    - Above CMC
2. With foam
    - Below CMC
    - Above CMC
    - Above CMC, line filter 0.5 μm
    - Above CMC, line filter 2.0 μm
    - Below CMC, using foaming loop
    - Above CMC, using foaming loop

The following few sections show the plots for the different experiments carried out. The plots include pressure versus time, temperature versus time and rate versus molar concentration data. The values of rate constant and order of the reaction are calculated using the plot of rate versus concentration of gas consumed. It should be noted that only a section of the whole reaction has been considered for the rate versus concentration plot. This includes a few points before and after the hydrate formation. The section has been circled for the case shown in Fig. 5.7.

Please note that association curves are shown in blue and dissociation in red, for all cases.

Experiment for hydrate formation without foam below CMC

There was **no hydrate formation** observed with below CMC concentration of SDS. The CMC of SDS is 0.0082 mol/L water (Israelachvili, 1991) which is 0.24 grams/100 mL water. The concentration used for this experiment is 0.2 grams/100 mL. The concentration of SDS used was deliberately chosen lower than its CMC to study the effect of the presence of micelles. This concept is explained in detail in the next chapter.

Experiment for hydrate formation without foam above CMC

Hydrate formation was observed in 230 minutes. The concentration of SDS used was 0.3 grams/100 mL. Comparing this experiment with the previous one, it can be observed that presence of micelles have a significant role in hydrate formation.

Figures 5.7 through 5.11 show the pressure versus time, temperature versus time and rate versus concentration of gas consumed and produced for hydrate association and dissociation respectively.

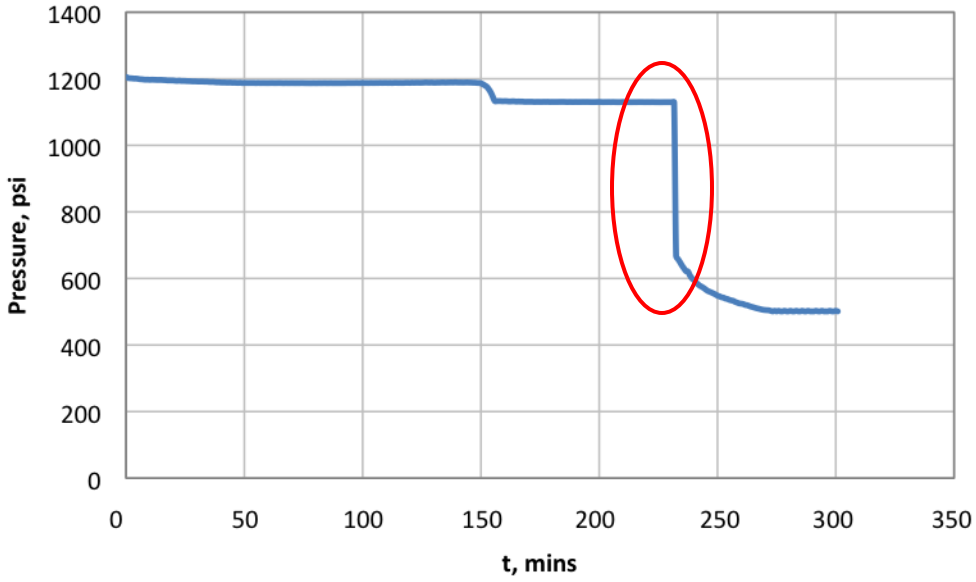

Figure 5.7: Pressure vs time for association of hydrates with SDS above CMC, without foam (Ellipse shows the section used for the rate vs consumption plot).

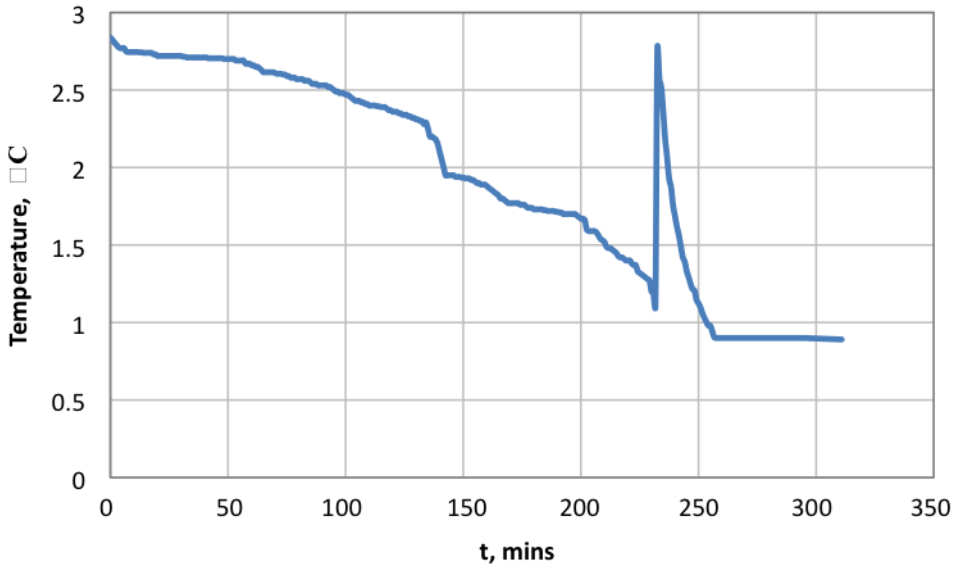

Figure 5.8: Temperature vs time for association of hydrates with SDS above CMC, without foam.

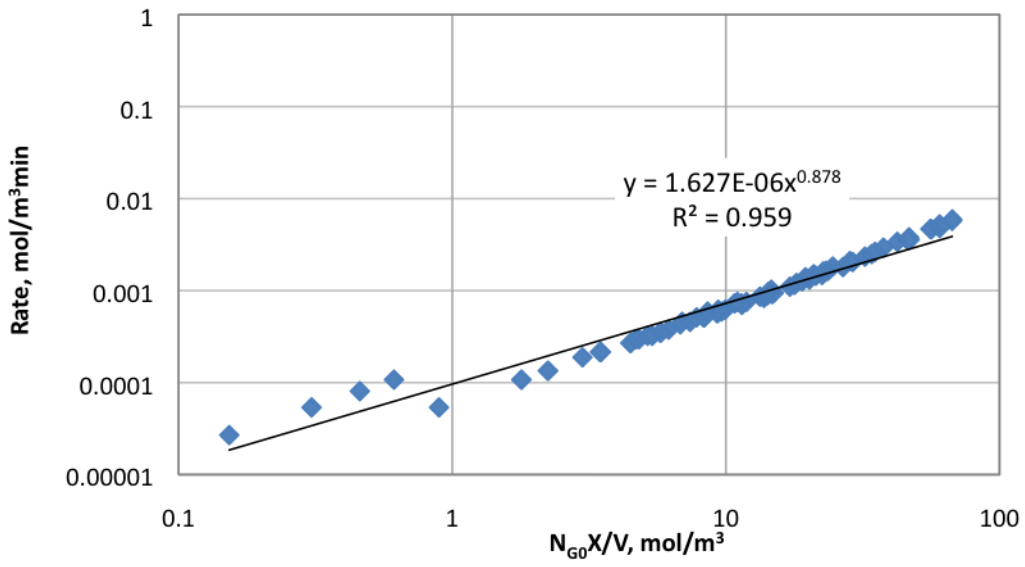

Figure 5.9: Rate vs concentration of gas consumed for association of hydrates with SDS above CMC, without foam.

From Figure 5.9,

Rate constant = 1.627×10^{-6} min^{-1}

Surface area exponent = 0.878

In the following plots, the variation of pressure and temperature with time, for the dissociation reaction are presented.

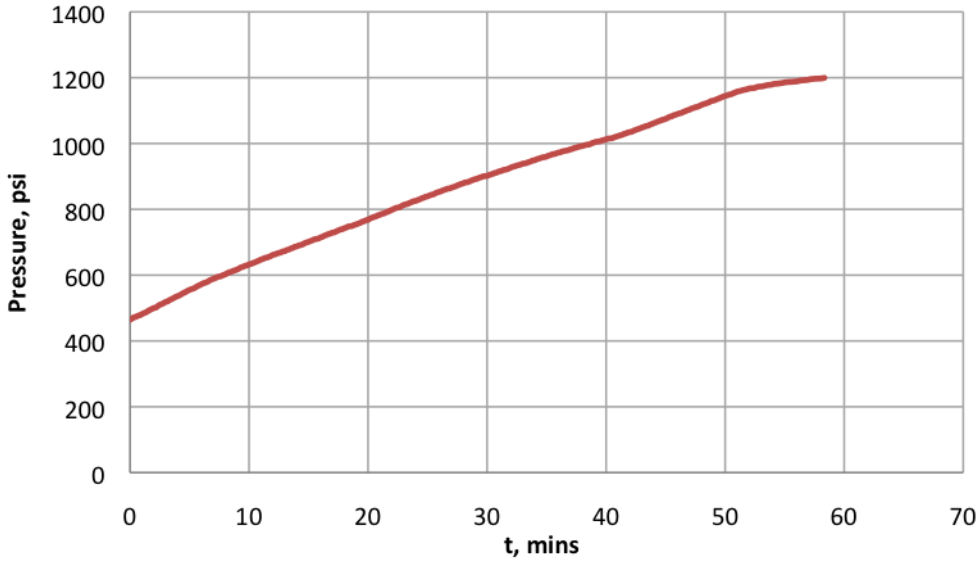

Figure 5.10: Pressure vs time for dissociation of hydrates with SDS above CMC, without foam.

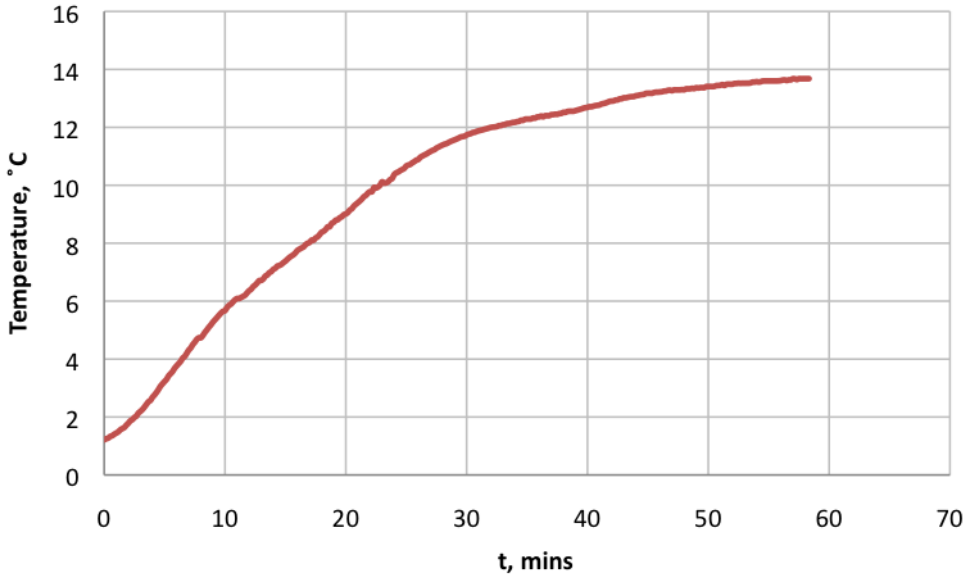

Figure 5.11: Temperature vs time for dissociation of hydrates with SDS above CMC, without foam.

Experiment for hydrate formation below CMC with foam

Figures 5.12 through 5.16 show the association and dissociation plots for the experiment with water and SDS with concentration below CMC, with foam. The amount of SDS used for this trial is 0.2 grams/100 mL.

Association of hydrates for this case took 180 minutes, a significant improvement when compared to the case without foaming where there was no hydrate formation. This establishes the important role played by foam during hydrate formation. In addition to this, the experiments presented henceforth consolidate this theory.

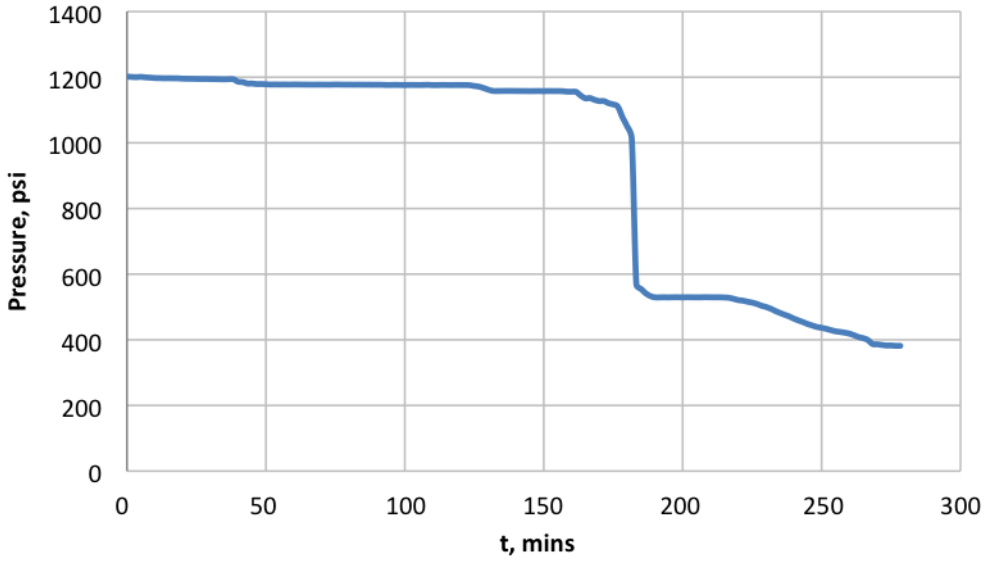

Figure 5.12: Pressure vs time for association of hydrates with SDS below CMC, with foam.

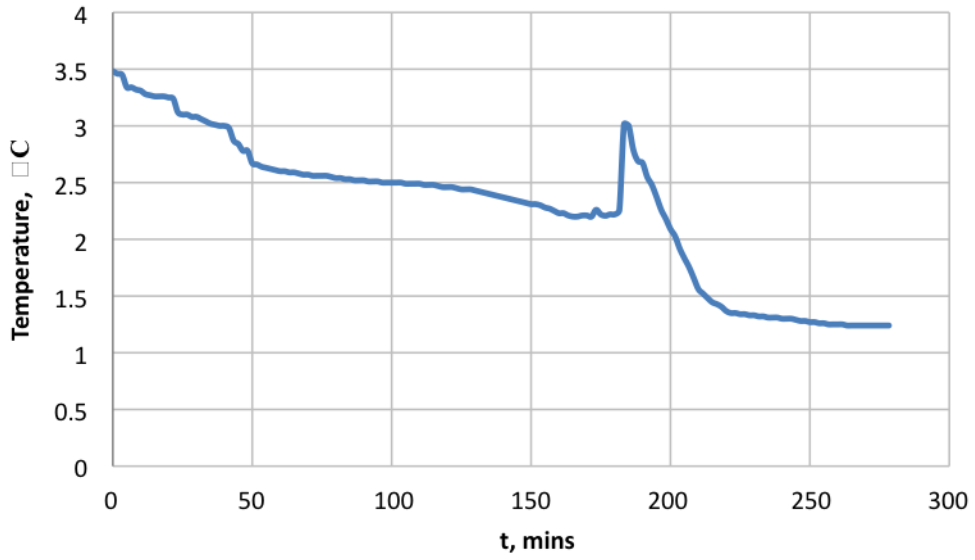

Figure 5.13: Temperature vs time for association of hydrates with SDS below CMC, with foam.

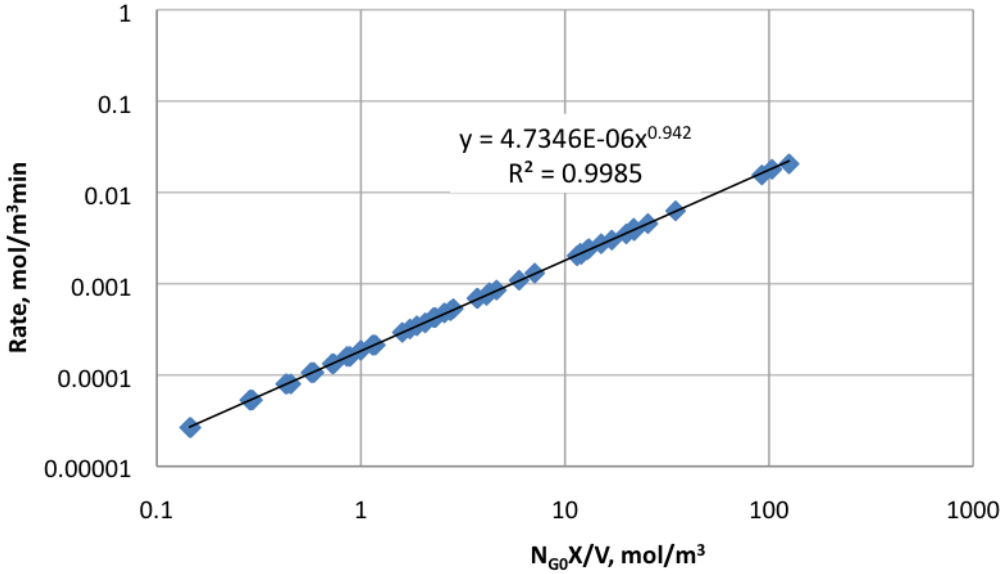

Figure 5.14: Rate vs concentration of gas consumed for association of hydrates with SDS below CMC, with foam.

From Figure 5.14,

Rate constant = 4.7346×10^{-6} min^{-1}

Surface area exponent = 0.942

Figures 5.15 and 5.16 show the dissociation curves for the hydrate reaction with SDS below CMC.

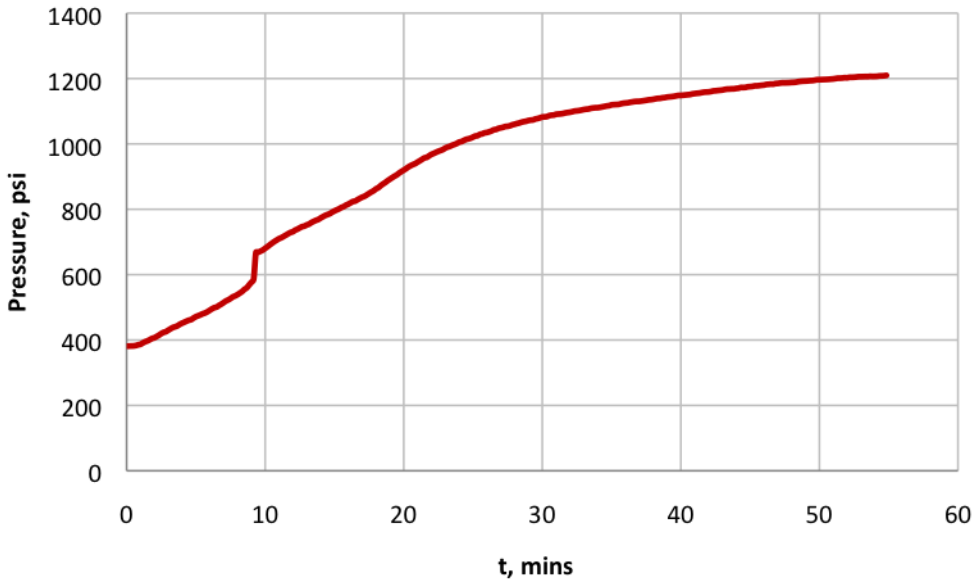

Figure 5.15: Pressure vs time for dissociation of hydrates with SDS below CMC, with foam.

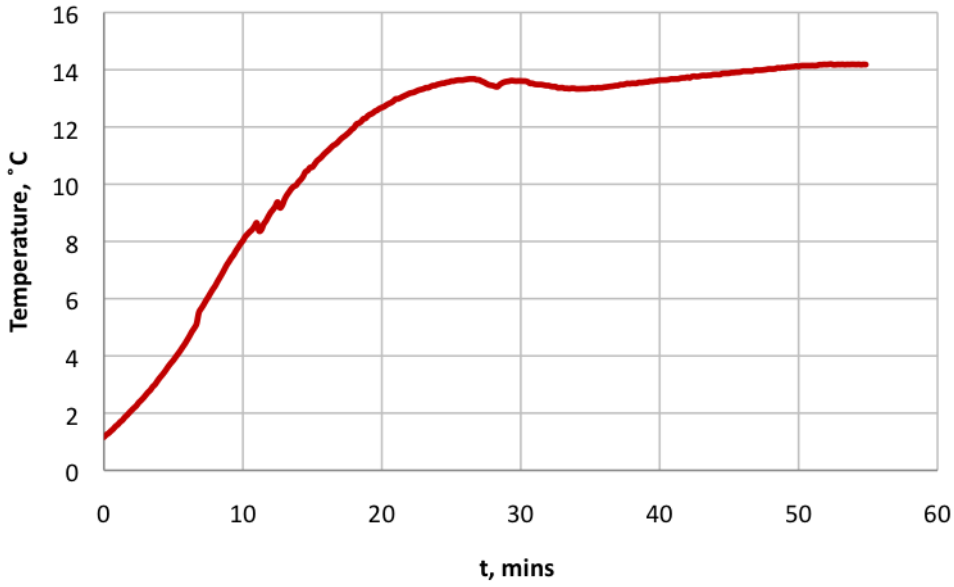

Figure 5.16: Temperature vs time for dissociation of hydrates with SDS below CMC, with foam.

Experiment for hydrate formation with foam above CMC

The time taken for hydrate formation in this case was 145 minutes. Among the experiments performed with foaming using just the hydrate cell, the time taken for hydrate formation is the least in this case.

Furthermore, the time taken is known to reduce further depending on the bubble size of the foam, which was tested by using foam of high quality and very small bubble size. The experiments showing the effect of bubble size are presented in the following sections.

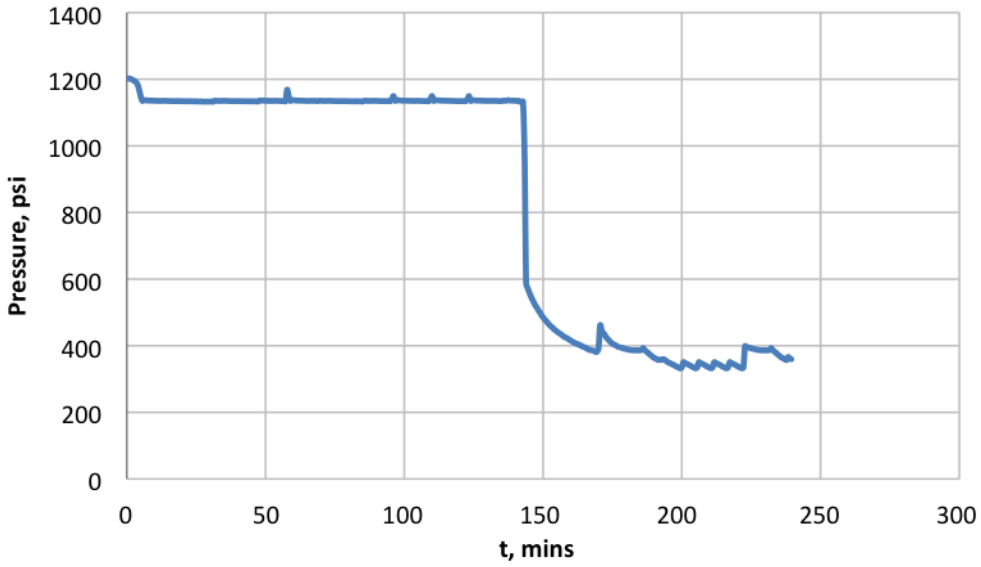

Figure 5.17: Pressure vs time for association of hydrates with SDS above CMC, with foam.

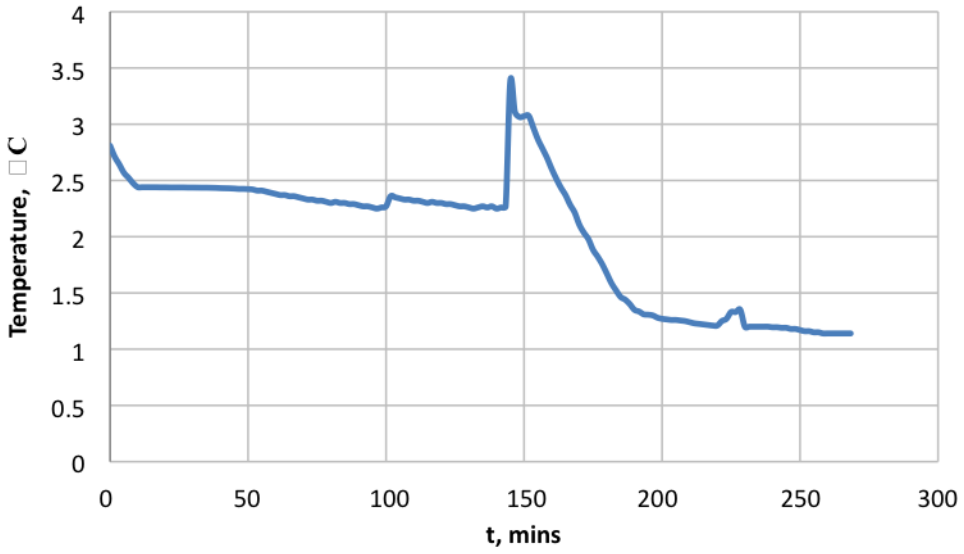

Figure 5.18: Temperature vs time for association of hydrates with SDS above CMC, with foam.

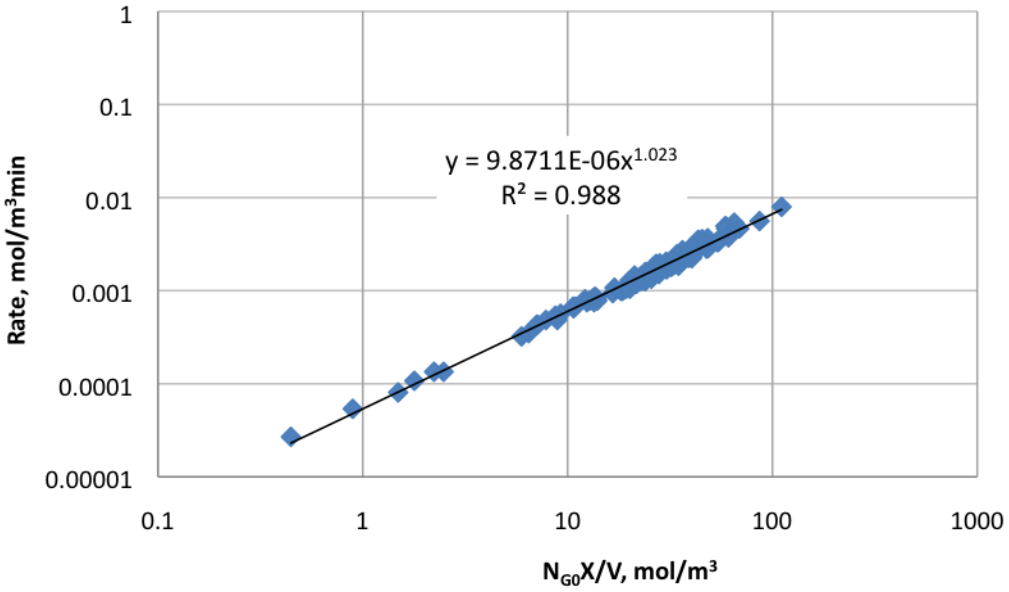

Figure 5.19: Rate vs concentration of gas consumed for association of hydrates with SDS above CMC, with foam.

From Figure 5.19,

Rate constant = 9.8711 x 10^{-6} min^{-1}

Surface area exponent = 1.023

The dissociation curves for this case are as follows.

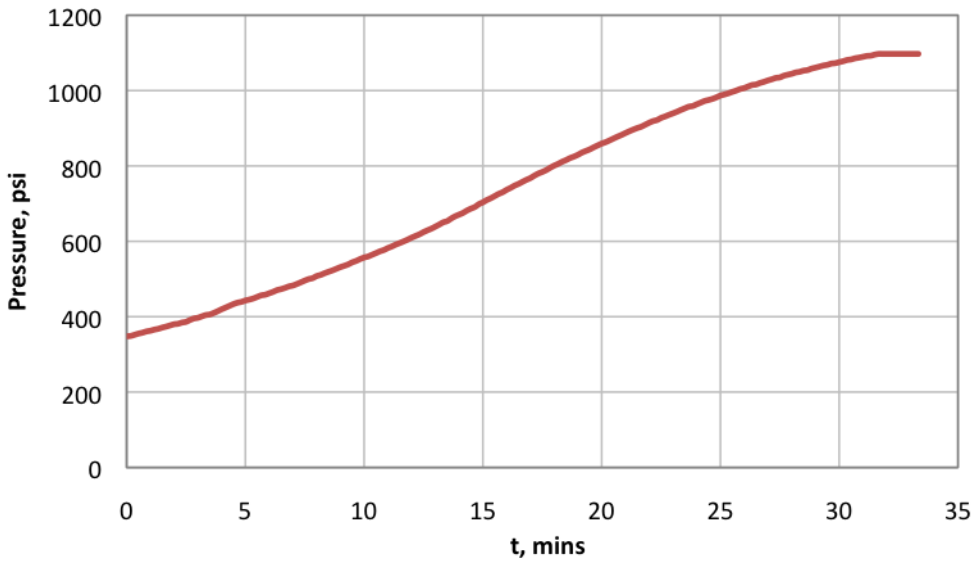

Figure 5.20: Pressure vs time for dissociation of hydrates with SDS above CMC, with foam.

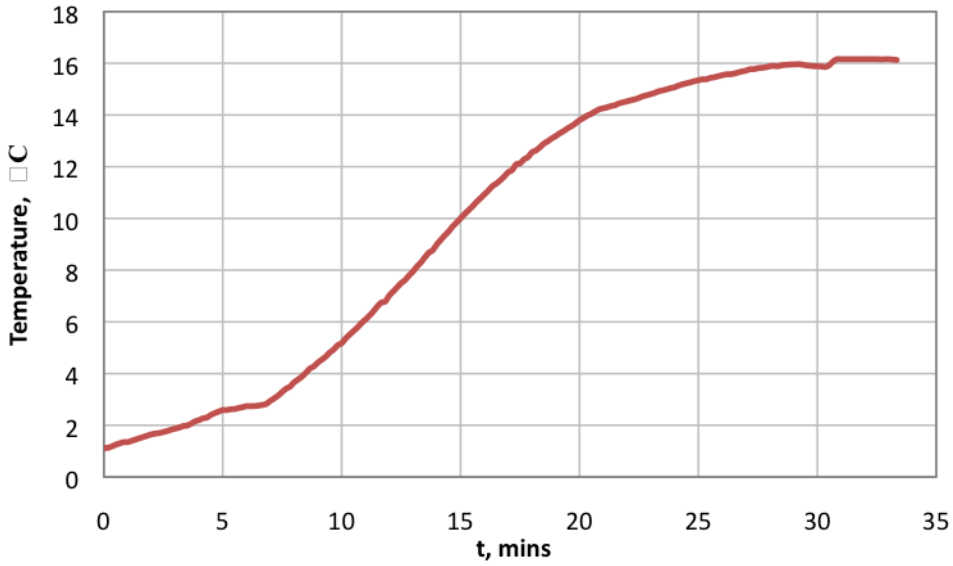

Figure 5.21: Temperature vs time for dissociation of hydrates with SDS above CMC, with foam.

Experiment for hydrate formation with foam above CMC, 0.5 µm filter

This experiment was performed to test the hypothesis that the bubble size has an effect on the induction time. All the previous experiments have been performed using 0.5 µm filter, so this experiment can be considered as a repetition of the experiment with foam above CMC. This experiment proves the reproducibility of the result. Two experiments were performed using 0.5 µm filter and 2.0 µm filter respectively. The increase in bubble size led to an increase in the induction time by more than an hour. This can be attributed to the decreased interfacial area of contact between gas and liquid due to an increase in bubble size. The time taken for hydrate formation with a 0.5 µm filter was 155 minutes, whereas the time taken with a 2.0 µm filter was 220 minutes.

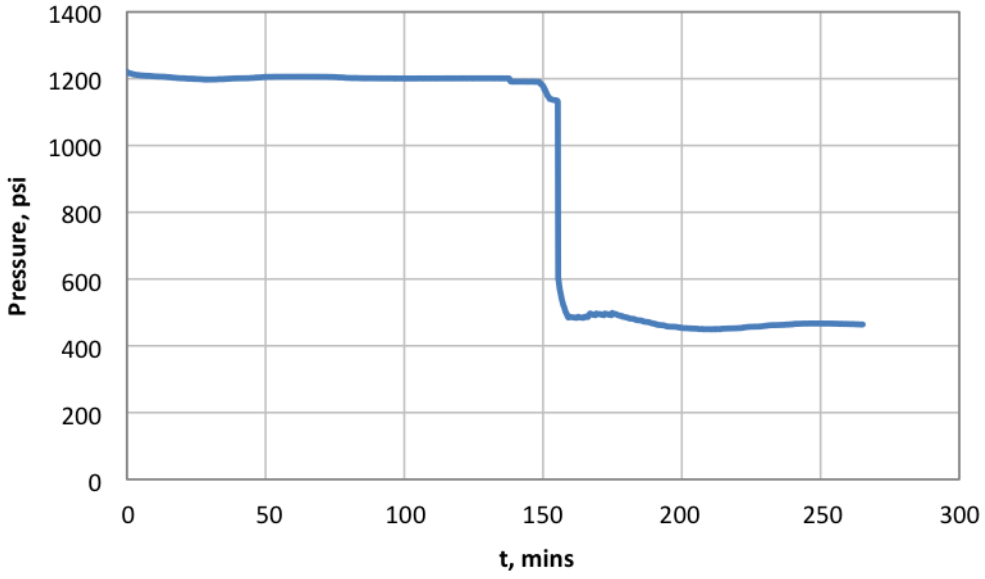

Figure 5.22: Pressure vs time for association of hydrates above CMC, with foam using 0.5 µm filter.

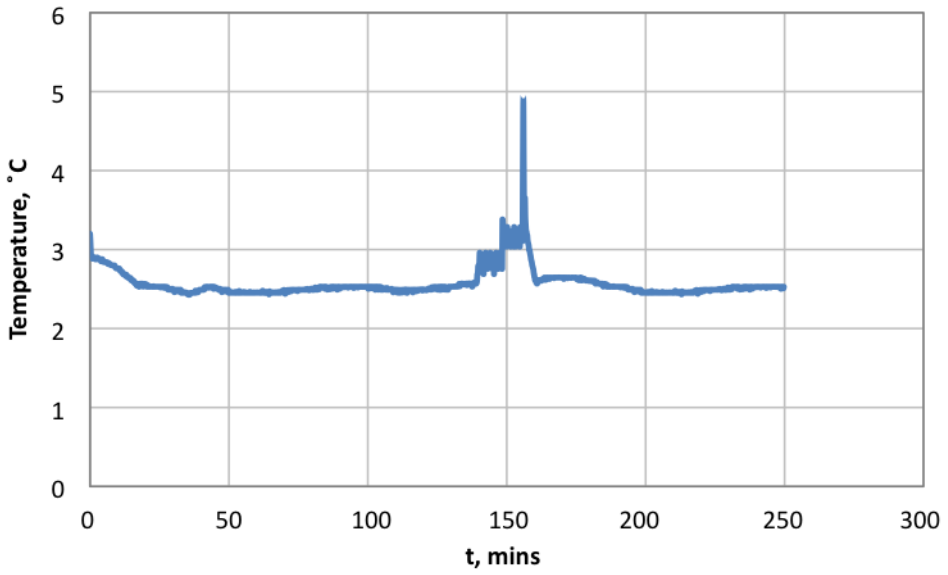

Figure 5.23: Temperature vs time for association of hydrates above CMC, with foam using 0.5 µm filter.

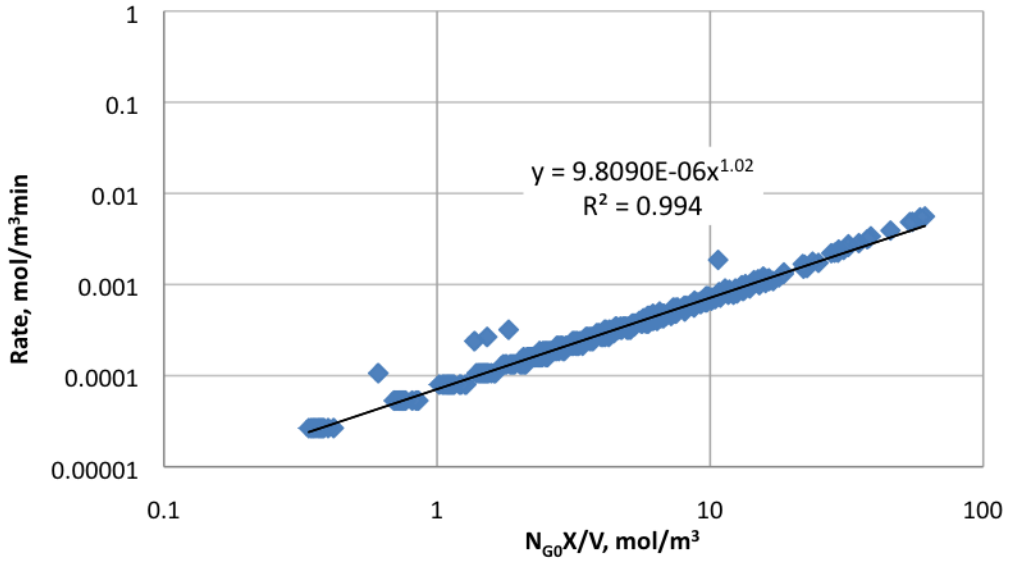

Figure 5.24: Rate vs concentration of gas consumed for association of hydrates above CMC, with foam using 0.5 µm filter.

From Figure 5.24,

Rate constant = 9.809 x 10^{-6} min^{-1}

Surface area exponent = 1.015

Dissociation plots have not been shown as it can be safely assumed that dissociation remains unaffected by this factor.

Experiment for hydrate formation with foam above CMC, 2.0 µm filter

This experiment shows the effect of size of bubbles in the foam when compared to the experiment with 0.5 µm filter. Figures 5.25 through 5.27 summarize the results for a 2.0 µm filter case.

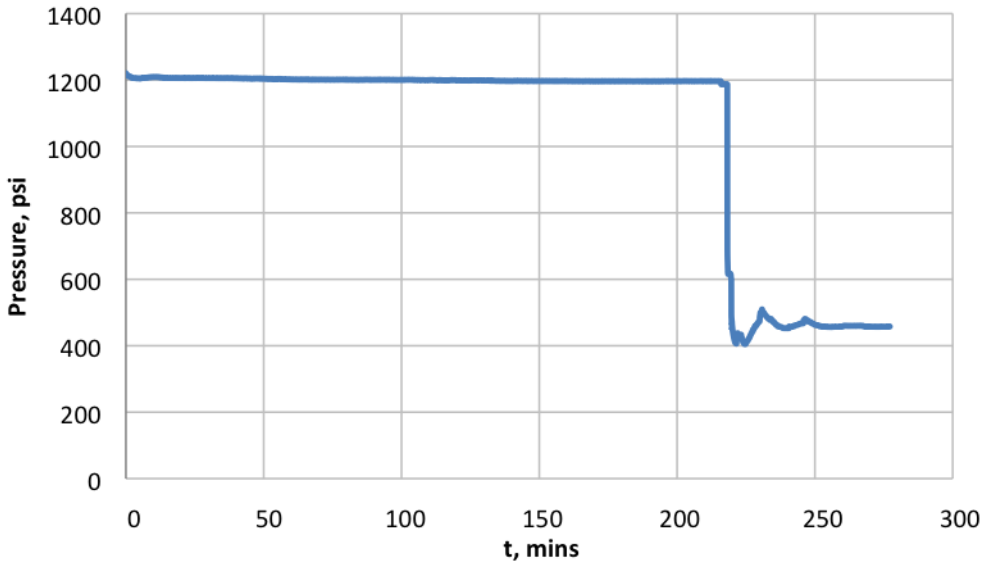

Figure 5.25: Pressure vs time for association of hydrates above CMC, with foam using 2.0 µm filter.

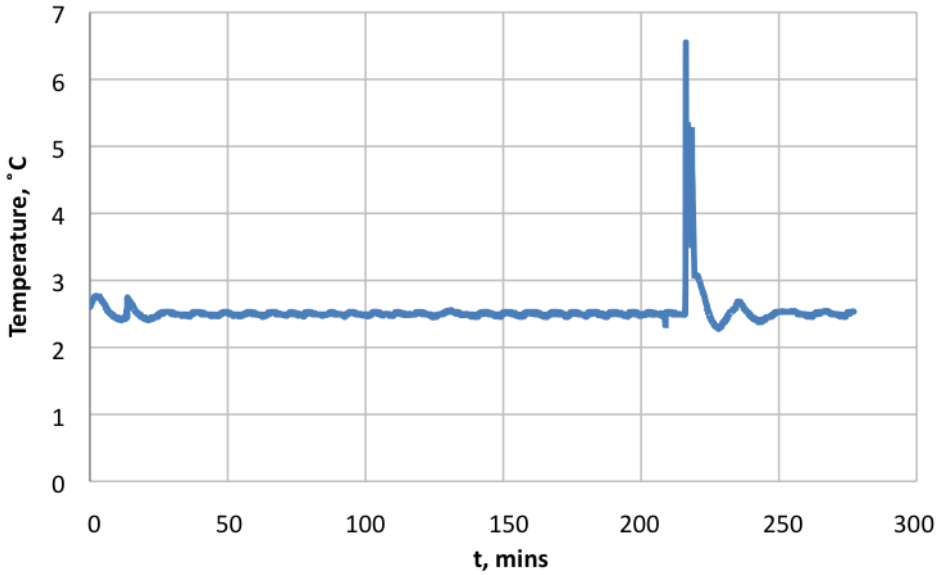

Figure 5.26: Temperature vs time for association of hydrates above CMC, with foam using 2.0 µm filter.

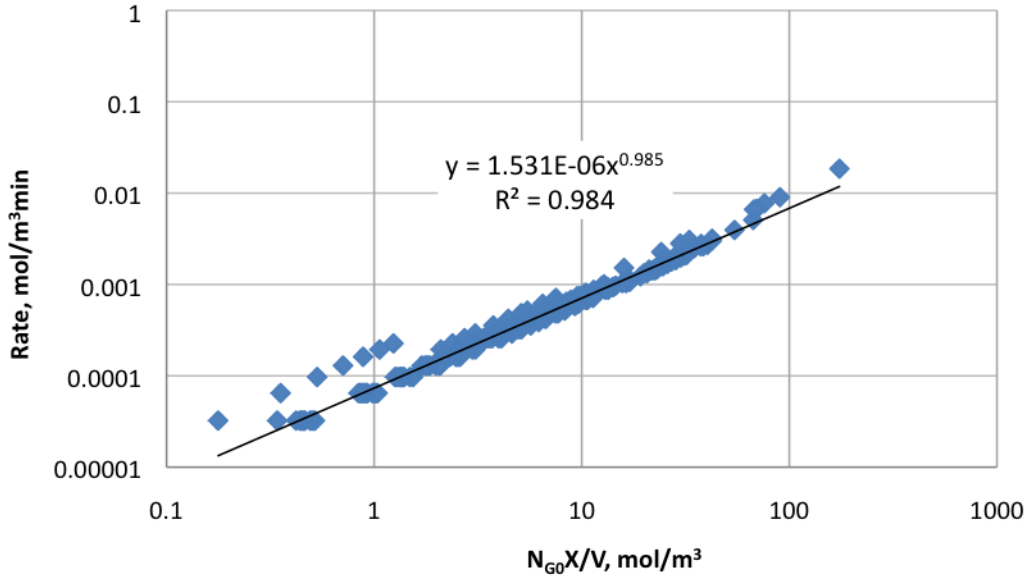

Figure 5.27: Rate vs concentration of gas consumed for association of hydrates above CMC, with foam using 2.0 µm filter.

From Figure 5.27,

Rate constant = 1.531×10^{-6} min^{-1}

Surface area exponent = 0.985

Experiment for hydrate formation with foam below CMC, using foaming loop

After noticing the significant effect of bubble size on induction time, experiments were performed using foam produced from a flow loop originally used for energized fluid leak off tests. This foam is of high quality (~ 65%). In layman terms, the foam in appearance is equivalent to shaving foam. The foam produced using this loop was then transferred into the hydrate cell, as explained in the previous chapter.

The time taken for hydrate formation reduced significantly. In this case, the time taken for hydrate formation is 115 minutes, whereas the time taken for the case of foaming with only the hydrate cell is 180 minutes.

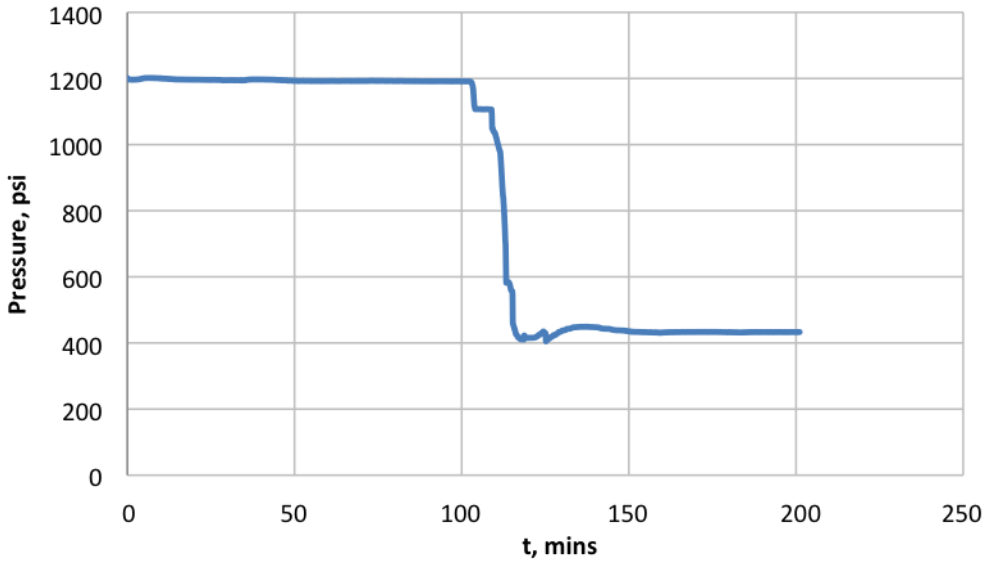

Figure 5.28: Pressure vs time for association of hydrates below CMC, using foaming loop.

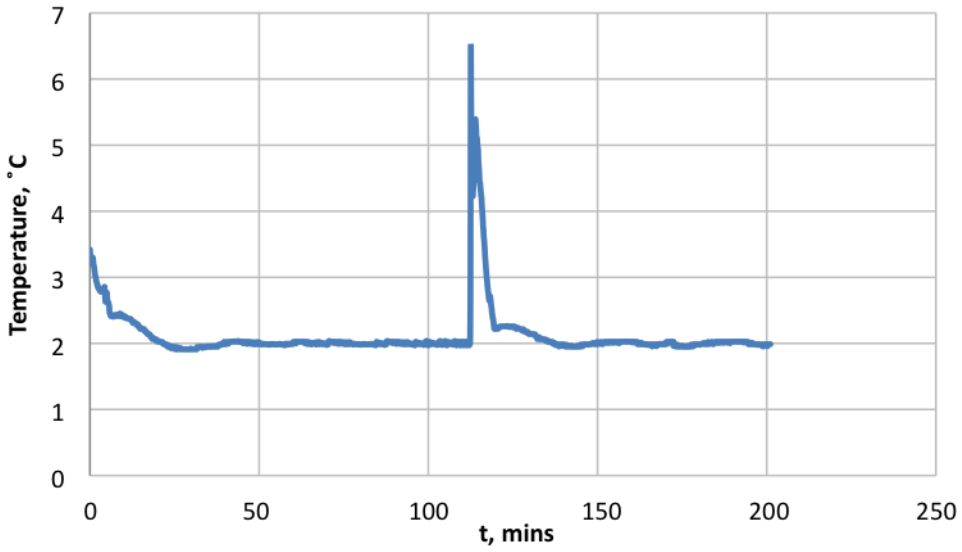

Figure 5.29: Temperature vs time for association of hydrates below CMC, using foaming loop.

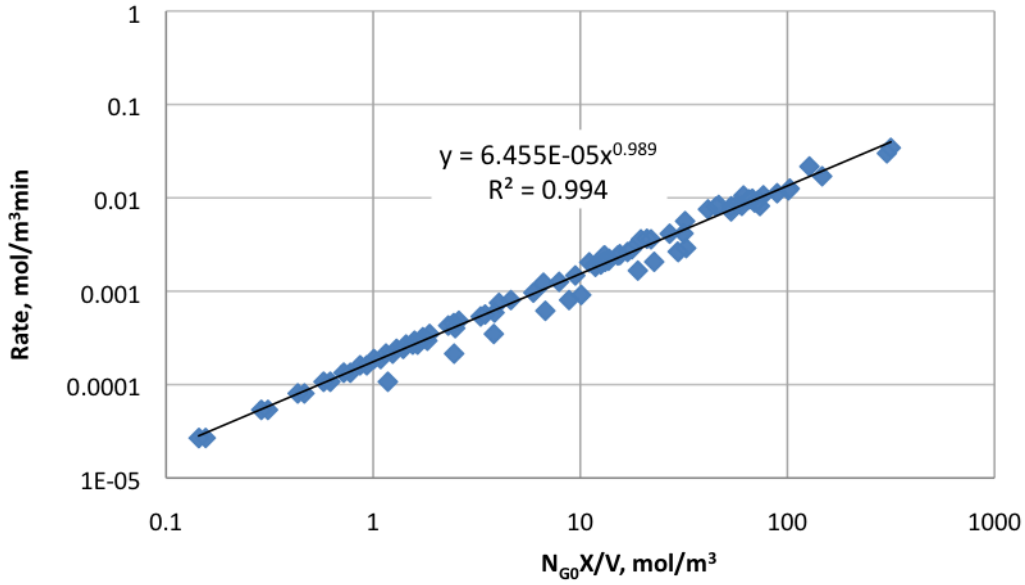

Figure 5.30: Rate vs concentration of gas consumed for association of hydrates below CMC, using foaming loop.

From Figure 5.30,

Rate constant = 6.455×10^{-5} min^{-1}

Surface area exponent = 0.989

Experiment for hydrate formation with foam above CMC, using foaming loop

The time taken for hydrate formation in this case is the least amongst all the experiments. Induction time was 80 minutes for this case whereas the time taken was 145 minutes for foam formation above CMC using just the hydrate cell.

From this experiment, it is deduced that both micelles and foam have significant roles to play in reducing the time taken for hydrate formation. These deductions are explained in detail in the next chapter.

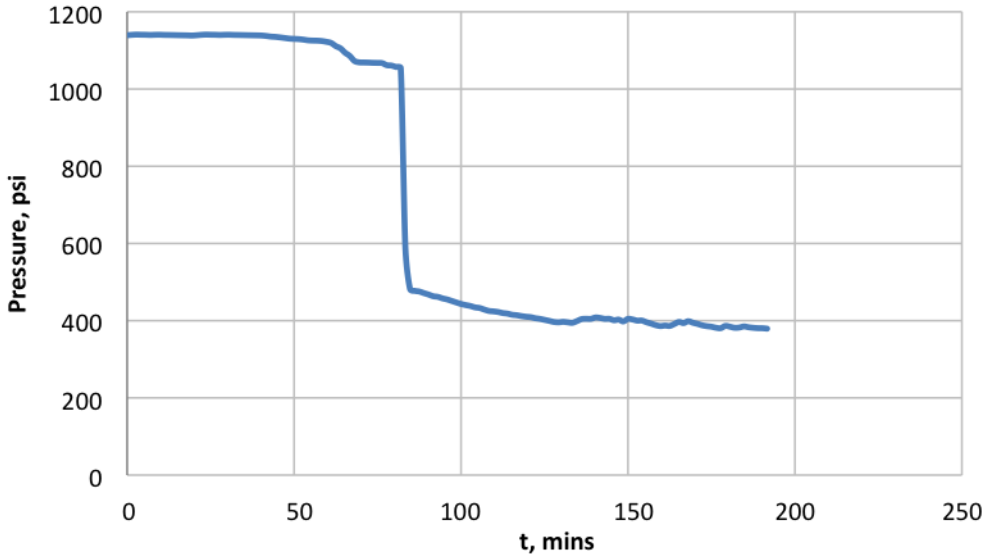

Figure 5.31: Pressure vs time for association of hydrates above CMC, using foaming loop.

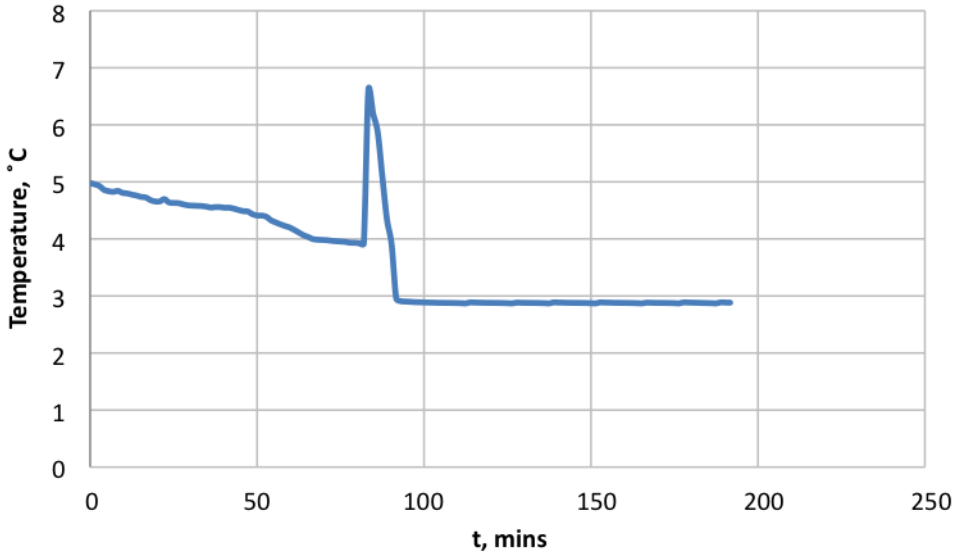

Figure 5.32: Temperature vs time for association of hydrates above CMC, using foaming loop.

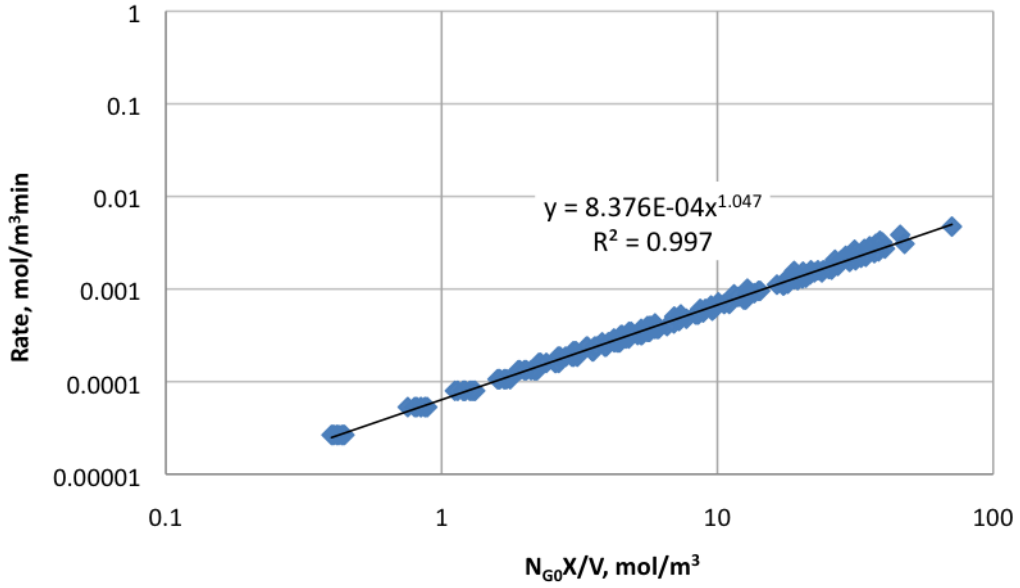

Figure 5.33: Rate vs concentration of gas consumed for association of hydrates above CMC, using foaming loop.

From Figure 5.33,

Rate Constant = 8.376×10^{-4} min^{-1}

Surface area exponent = 1.047

Tables 5.1 and 5.2 summarize the association reactions in terms of their induction times and rate constants.

	SDS Concentration	Filter size (μm)	Foaming method	Induction Time (mins)
Without foam	Below CMC	0.5		No Hydrates
	Above CMC	0.5		230
With foam	Below CMC	0.5	Hydrate Cell	180
			Foaming Set-up	120
	Above CMC	0.5	Hydrate Cell	150
		2.0	Hydrate Cell	220
			Foaming Set-up	80

Table 5.1: Induction times for different association experiments using SDS.

	SDS Concentration	Filter size (μm)	Foaming method	Rate Constant (min^{-1})
Without foam	Below CMC	0.5		No Hydrates
	Above CMC	0.5		1.627×10^{-6}
With foam	Below CMC	0.5	Hydrate Cell	4.735×10^{-6}
			Foaming Set-up	6.455×10^{-5}
	Above CMC	0.5	Hydrate Cell	9.800×10^{-6}
		2.0	Hydrate Cell	1.531×10^{-6}
			Foaming Set-up	8.376×10^{-4}

Table 5.2: Rate constants for different association experiments using SDS.

In summary,

1. **Effect of concentration of SDS is pronounced**: The experiments with concentration of SDS above CMC take lesser time as compared to the ones with the below CMC concentrations. The varying effect is shown in the form of a bar graph in Fig 5.34.
2. **Foaming plays an important role**: The experiments carried out using the foaming method, initially, using just the hydrate cell and then the foaming loop show consistent reduction in the induction time.
3. **And, the bubble size of the foam is important**: Aside from the fact that foaming helps in reducing the induction time, the size of the bubbles in the foam play an important part too (Fig. 5.35). The smaller the bubble size .i.e. the finer the foam, the lesser the time taken for hydrate formation.

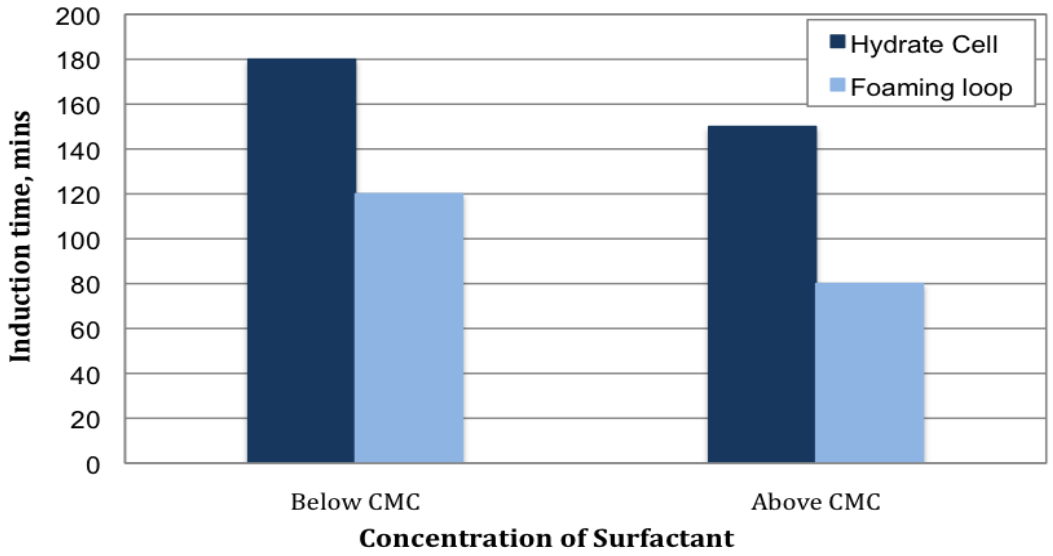

Figure 5.34: Variation of induction time with respect to concentration of the surfactant.

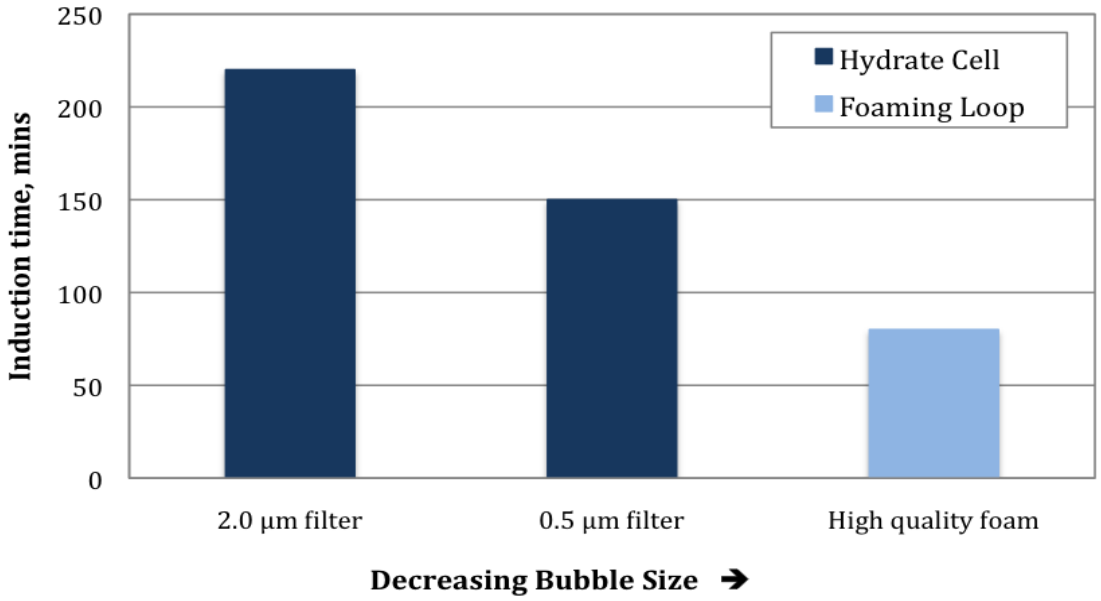

Figure 5.35: Variation of induction time with respect to bubble size of foam (above CMC).

From these observations, it is inferred that micelle concentration, foaming and bubble size of foam play very important roles in formation of hydrates. These conclusions are explained in detail in the upcoming chapter.

5.3.3. Cetyl Trimethylammonium Bromide (CTAB)

Different trials were performed using CTAB. Both, concentrations above and below the CMC of CTAB had an inhibiting effect on the formation of hydrates. After gas and water injection, the set-up was allowed to rest for up to 6 days for a few experiments, but there was no formation. Gas was injected at pressures of 1200 psi for the initial cases, but was then increased to 1500 psi to encourage hydrate formation. Increasing the initial pressure had no effect as well.

5.3.4. Alpha Olefin Sulfate

Like SDS, Alpha Olefin Sulfate (AOS) is also an anionic surfactant, but AOS, used in different concentrations, did not aid hydrate formation.

Chapter 6: Analysis of Results

It can be deduced from the induction time and the values of rate constant obtained from the experiments that the following factors play an important role in aiding hydrate formation.

1. Presence of micelles to serve as nucleation sites
2. Presence of foam which increases the interfacial area of contact between gas and liquid.

6.1. IMPORTANCE OF SURFACTANT CONCENTRATION

6.1.1. What are micelles?

Micelles are colloidal aggregates of surfactant molecules that form in a surfactant solution at and above a well-defined concentration known as the Critical Micelle Concentration (CMC). Also, micelle formation depends on a certain temperature called Krafft Temperature, which is the minimum temperature at which the solubility of the surfactant monomer becomes high enough for the surfactant to start forming micelles. Depending on the type of surfactant, the micellar structure formed varies. The possible aggregate structures are spherical micelles, worm-like micelles, spherical vesicles, lamellar sheets etc. The shape and size of a micelle is generally a function of the molecular geometry of the surfactant molecules. It also depends on the properties of the solution (concentration of surfactants, temperature, pH and ionic strength). The molecules undergo this process of aggregation to minimize the free energy of the solution.

Thus, a micellar solution is a colloidal dispersion of surfactant molecules that form aggregates to minimize the solution Gibbs free energy. In the case of a non-ionic

surfactant, the molecules cluster together in micelles of several hundred molecules, unlike their ionic counterparts, in which case this is not possible due to electrostatic repulsions between head groups. Ionic surfactants form aggregates of up to hundred molecules.

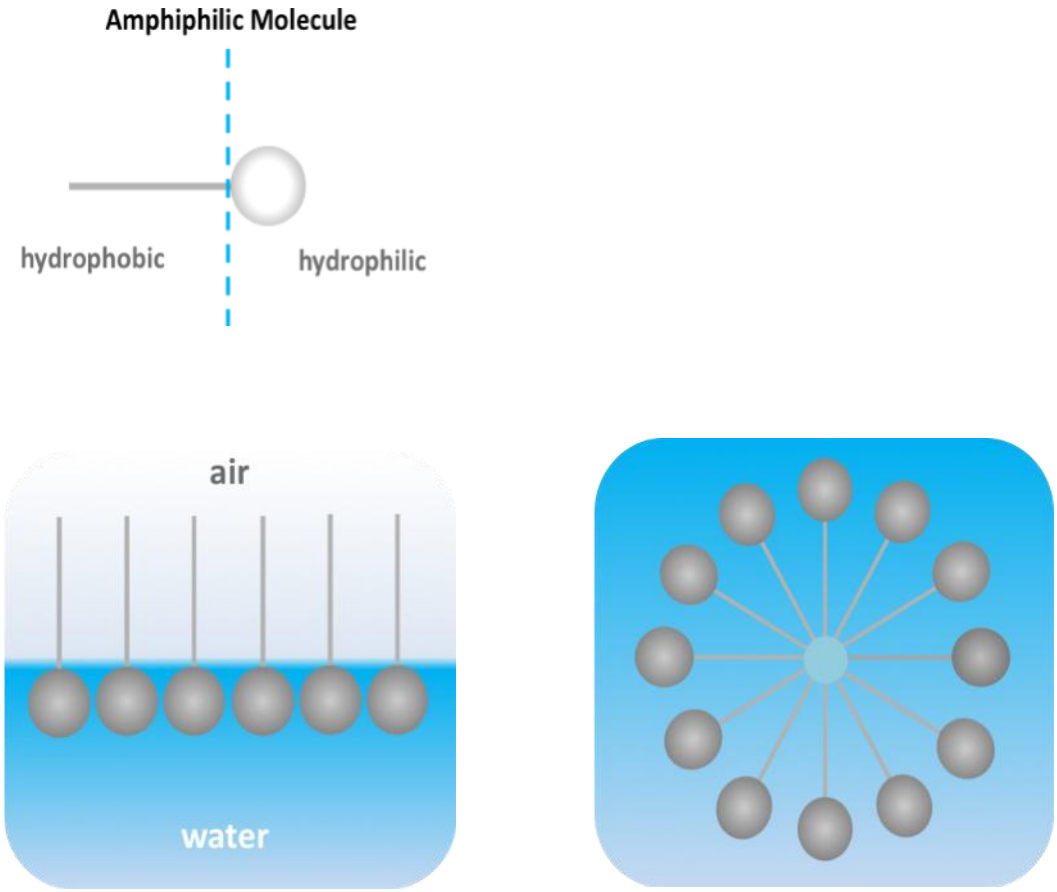

Figure 6.1 Micellar structure of an amphiphilic molecule.

6.1.2. Effect of micelles on hydrate formation

The experiments clearly show that SDS aids in the formation of hydrates. More than just the presence of the surfactant, the concentration of surfactants is of key importance. And by concentration of surfactants, specifically the presence of micelles is

considered as the significant participant. Hydrate formation, in general follows a mechanism of nucleation on certain regions called the nucleation sites. After these experiments, it was concluded that micelles, non-spherical in this case, serve as nucleation sites for the gas to accumulate and water to envelope it.

Micelles formed by SDS have been extensively studied and it has been found that this surfactant in water forms slightly non-spherical micelles. This was shown by Israelachvili (1991) as follows.

CMC of SDS = 0.0082 M

Aggregation Number = 62

Aggregation number is the number of molecules present in a micelle once CMC is reached.

Let l_c be the critical chain length in nanometers and n be the number of carbon atoms.

From calculations,

$$l_c \approx (0.154 + 0.1256n) \tag{6.1}$$

Hydrocarbon volume (in nanometers),

$$v = (27.4 + 26.9n) \times 10^{-3} \tag{6.2}$$

Mean aggregation number

$$M = \frac{4\pi R^2}{a_o} = \frac{4\pi R^3}{3v} \tag{6.3}$$

where,

$$R = \frac{3v}{a_o}$$

a_o is the optimal area.

Packing parameter for spherical packing is given as

$$\frac{v}{a_o l_c} < \frac{1}{3} \tag{6.4}$$

For SDS, the values of *M* and *n* were obtained from the literature as

$$M = 74$$
$$n = 12$$

Lipid	Critical packing parameter $v/a_0 l_c$	Critical packing shape	Structures formed
Single-chained lipids (surfactants) with large head-group areas: *SDS in low salt*	< 1/3	Cone 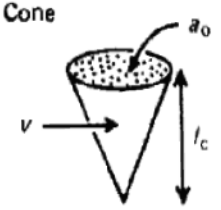	Spherical micelles 
Single-chained lipids with small head-group areas: *SDS and CTAB in high salt, nonionic lipids*	1/3-1/2	Truncated cone 	Cylindrical micelles 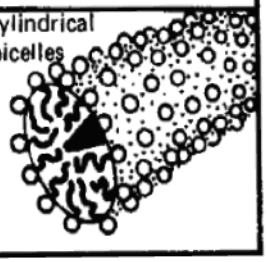

Table 6.1: Mean Packing Shapes and Structures (Israelachvili, 1991).

Upon calculating v, l_c, a_o, we obtain the value of packing parameter as 0.37, which is greater than $\frac{1}{3}$, and hence the slightly non-spherical micelles.

6.1.3. Importance and Purpose of Nucleation Sites

Heterogeneous nucleation is far more commonplace when compared to homogeneous nucleation, as stated before. Heterogeneous nucleation takes place in the presence of foreign bodies such as dust particles, fluid interface or container walls. From a free energy point of view, it has been found that it is easier to form hydrate nuclei in a two dimensional surface like dust or container wall, rather than a three dimensional surface-free volume of water (Sloan and Koh, 2007). In the case of heterogeneous nucleation, the presence of these foreign particles reduces the excess free energy and the critical radius required to form crystal clusters of hydrates.

From the experiments conducted and the knowledge on the micelles formed by SDS, it was concluded that these non-spherical micelles serve as "foreign particles" that act as nucleation sites. This reduces the excess energy required to form hydrate crystals, and bring down the induction time by a significant factor.

6.2. IMPORTANCE OF GAS-LIQUID INTERFACE

It was concluded by Long (1994) and Kvamme (1996) that nucleation occurs at the interface of the liquid and gas, specifically on the gas side of the interface. This implies that the interfacial area between gas and liquid, in this case water (or water-surfactant solution) and methane contributes significantly to the nucleation process. A greater surface area acts as the driving force for hydrate crystal formation. Previous work (Vysniauskas and Bishnoi, 1982) states that gas gets adsorbed through surface diffusion and water molecules cage around the adsorbed species. For this adsorption to take place, the gas molecules must migrate to suitable locations that are in the vicinity of foreign particles that would assist in inducing nucleation. Labile clusters have then been noticed to join and grow on the gas side. In this light, it can be explained that the presence of foam increases the gas-liquid interfacial contact area and along with the presence of

foreign particles, like dust, container walls or micelles allows for faster paths to nucleation. Quantitative analysis of the effect of increase in gas-liquid interfacial area has not been carried out in this work.

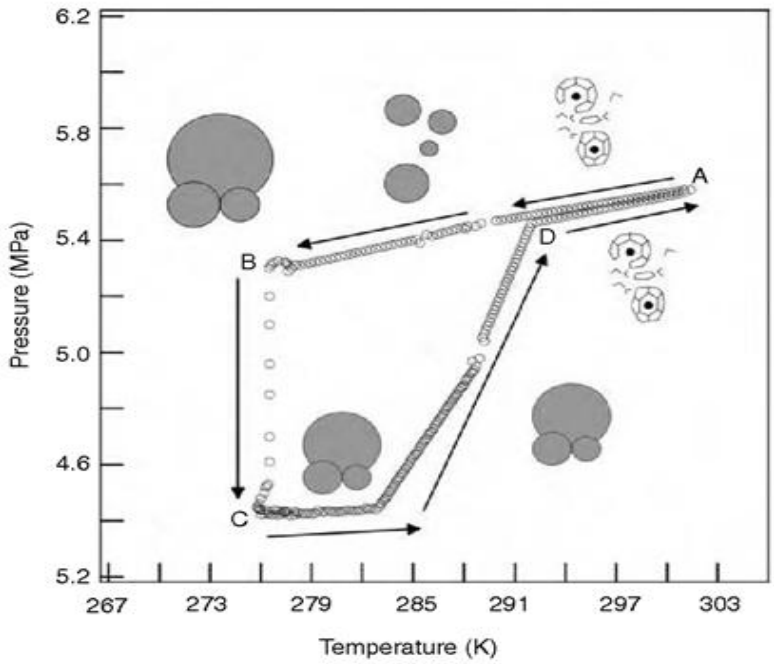

Figure 6.2: Hydrate Labile Cluster Growth (Christiansen et al., 1994).

6.3. MISCELLANEOUS OBSERVATIONS AND INFERENCES

1. Micelle Experiment - A micelle differentiation experiment was conducted by making the SDS solution a little basic to allow spherical micelles to form (Israelachvili, 1991). This was done to check if a different geometry of micelles has any effect on hydrate formation kinetics. Unfortunately, there was no formation of hydrates for this experiment and it could not be concluded whether this was due to the modified micelle geometry or the basicity which inhibited the reaction.

2. Methane of high purity - After a few non-reproducible attempts and unsuccessful trials, the purity of methane was considered. The 99% purity that was being used was replaced with 99.99% ultra pure methane. This change led to positive and reproducible results for cases that were previously unsuccessful. This is believed to be due to certain impurities present in the 99% pure methane that might have acted as inhibitors.
3. Using vacuum pump - Use of a vacuum pump to rid the cell of unwanted pockets of air is an important step that was taken before conducting any experiment.
4. Formation of hydrates along the walls - As discussed in the previous section, presence of nucleation sites (foreign particles) is a major factor in formation of methane hydrates. It was found from the experiments that, hydrates indeed formed on the walls of the container as stated by Sloan and Koh (2007).
5. Formation of hydrates at lower pressures - The initial experiments conducted without using the foaming loop required pressures of 1200 psi and above for the hydrates to form. On the other hand, it was noticed that with foam from foaming loop, hydrates formed at pressures of 850 psi and above.

Chapter 7: Conclusion

The experiments performed suggest that the presence of the sodium dodecyl sulfate (SDS) surfactant aids the formation of methane hydrate. There was a significant reduction in the induction time between the experiments performed with the concentration of SDS above and below CMC. The experiments conducted with SDS above CMC took lesser time as compared to the ones performed using concentrations below its CMC. From this result, it has been deduced that the presence of nucleation sites in the form of micellar structures play a significant role.

Foaming, which was initially carried out using just a line filter, had a pronounced effect on the induction time. It was also noticed that the induction time was directly related to the size of the bubble. Based on these observations, experiments were carried out using high quality foam (~65%). The foam was produced by periodically injecting gas in a flow loop with a circulating pump. The induction time for hydrate formation was reduced to 80 minutes from the initial induction time of more than 250 minutes. A series of similar experiments confirmed the reproducibility of this result.

In addition to this, the kinetics of association of methane hydrates were calculated from the experimental data. In terms of dissociation, there was no significant difference in the results for different concentrations of the same surfactant or for different surfactants.

In summary, it can be concluded that

1. The association reaction is diffusion controlled.
2. The concentration of the SDS surfactant (above the critical micelle concentration) has a significant effect on the induction time due to the presence of micelles.

3. Foam aids the association reaction significantly by increasing the interfacial area between gas and liquid. The bubble size of the foam also plays an important role as smaller bubble sizes mean more interfacial area of contact.
4. There was no significant difference in the dissociation kinetics with surfactant or foam.
5. CTAB was found to be an effective inhibitor, both above and below its CMC.

References

Bin, D., Guosheng, J., Xiang, W., Fenglin, Tang. "Research of Surfactants Effect on Methane Hydrate Formation." SPE International Oil & Gas Conference and Exhibition, Beijing (2006): SPE 103689.

Bishnoi, P.R., Natarajan, V. "Formation and Decomposition of Gas Hydrates." Fluid Phase Equilibria 117 (1996), pp. 168-177.

Christiansen, R.L., Sloan, E.D. "Mechanism and Kinetics of Hydrate Formation." Annals of the New York Academy of Sciences 715 (1994), pp. 283-305.

Claussen, W.F. "A Second Water Structure for Inert Gas Hydrates." J. Chem. Phys. 19, 11 (1951), pp. 1425.

Claussen, W.F., Polglase, M.F. "Solubilities and Structures in Aqueous Aliphatic Hydrocarbon Solutions." J. Am. Chem. Soc. 74, 19 (1952), pp. 4817-4819.

Davy, H. Phil. Trans. Roy. Soc. Lond. 101 (1811).

Englezos, P., Kalogerakis, N., Dholabhai, P.D., Bishnoi, P.R. "Kinetics of formation of Methane and Ethane Gas Hydrates." Chem. Sci. Eng. 42 (1987), pp. 2647-2658.

Englezos, P., Kalogerakis, N., Bishnoi, P.R. "Formation and Decomposition of Gas Hydrates of Natural Gas Components." Journal of Inclusion Phenomena and Molecular recognition in Chemistry 8 (1990), pp. 89-101.

Ganji, H., Manteghian, M., Mofrad, H.R. "Effect of Mixed Compounds on Methane Hydrate Formation and Dissociation Rates and Storage Sapacity." Fuel Processing Technology 88 (2007) 891-895.

Gnanendran, N., Amin, R. "The Effect of Hydrotropes on Gas Hydrate Formation." Journal of Petroleum Science & Engineering 40 (2003), pp. 37-46.

Gudmundsson, J.S., Parlaktuna, M. "Storage of Natural Gas Hydrates at Refrigerated Conditions." AIChE Spring National Meeting, New Orleans (1992).

Gudmundsson, J.S., Parlaktuna, M., Khokhar, A.A. "Storing Natural Gas as Frozen Hydrate." SPE Production and Facilities 9, 1 (1994), pp.69-73.

Gudmundsson, J.S., Hveding, H., Borrehaug, A. "Transport of Natural Gas as Frozen Hydrate." Proc. Fifth International Offshore & Polar Engineering Conference, The Hague, 282 (1995).

Gudmundsson, J.S., Borrehaug, A. "Formation Rate of Methane and Mixture Hydrate." Proc. Second International Conference on Gas Hydrates, Toulouse, 415 (1996).

Hammerschimdt, E.G. "Formation of Natural Gas Hydrates in Transmission Lines." Ind. Eng. Chem. 26 (1934), pp. 851-855.

Israelachvili, J. 1991. Intermolecular & Surface Forces. 2nd ed: Academic Press.

Kalogerakis, N., Jamaluddin, A.K.M. "Effect of Surfactants on Hydrate Formation Kinetics." SPE International Symposium on Oilfield Chemistry, New Orleans (1993): SPE 25188.

Kanda, H. 2006. "Economic Study on Natural Gas Transportation with Natural Gas Hydrate Pellets." 23rd World Gas Conference, Amsterdam.

Kashchiev, D., Firoozabadi, A. "Driving Force for Crystallization of Gas Hydrates." Journal of Crystal Growth 241 (2002a), pp. 220-230.

Kashchiev, D., Firoozabadi, A. "Nucleation of Gas Hydrates." Journal of Crystal Growth 243 (2002b), pp. 476-489.

Kashchiev, D., Firoozabadi, A. "Induction Time in Crystallization of Gas Hydrates." Journal of Crystal Growth 250 (2003), pp. 499-515.

Kim, N.J., Lee, J.H., Cho, Y.S., Chun, W. "Formation Enhancement of Methane Hydrate for Natural Gas Transport and Storage." Energy 35 (2009), pp. 2717-2722.

Kvenvolden, A.K. "Gas Hydrates – Geological Perspective and Global Change." Rev. Geophys. 31 (1993), pp. 173-187.

Lederhos, J.P., Long, J.P., Sum, A., Christiansen, R.L., Sloan, E.D. "Effective Kinetic Inhibitors for Natural Gas Hydrates." Chem. Eng. Sci. 51 (1996), pp. 1221-1229.

Lekse, J., Taylor, C.E. "Effect of bubble size and density on methane conversion to hydrate." Journal of Petroleum Science & Engineering 56 (2007), pp. 97-100.

Levenspiel, O. 1998. Chemical Reaction Engineering: John Wiley & Sons.

Lin, W., Chen. G.-J., Sun, C.-Y., Guo, X.-Q., Wu, Z.-K., Liang, M.-Y., Chen, L.-T., Yang, L.-Y. "Effect of Surfactant on the Formation and Dissociation Kinetic Behavior of Methane Hydrate." Chemical Engineering Science 59 (2004), pp. 4449-4455.

Makogon, Y.F. "Natural gas Hydrates: Discovery and Prospect." Gazov. Prom-st. 5, 14 (1965).

Makogon, Y.F. 1997. Hydrates of Hydrocarbons: Penwell Publishing Company.

Makogon, Y.F., Makogon, T.Y., Holditch, S.A. "Kinetics and Mechanisms of Gas Hydrate Formation and Dissociation with Inhibitors." Annals of the New York Academy of Sciences 912 (2000), pp. 777-796.

Nogami, T., Shigeru, W. "Development of Natural Gas Supply Chain by Means of Natural Gas Hydrate (NGH)." International Petroleum Technology Conference (2008).

Ouar, H., Cha, S.B., Wildeman, T.R., Sloan, E.D. "Formation of gas Hydrates in Water-based Drilling Fluids." Trans I Chem. E. 70A (1992), pp. 48.

Pakulski, M. “Accelerating Effect of surfactants on Gas Hydrates Formation.” SPE International Symposium on Oilfield Chemistry, Houston (2007): SPE 106166.

Pauling, L., Marsh, R.E. “The Structure of Chlorine Hydrates.” Proc. Natl. Acad. Sci. 38, 2 (1952), pp. 112-118.

Sloan, E.D., Koh, C.A. 2007. Clathrate Hydrate of Natural Gases. 3rd ed: CRC Press.

Sun, Z.-G., Wang, R., Ma, R., Guo, K., Fan, S. “Natural gas storage in hydrates with the presence of promoters.” Energy Conversion and Management 44 (2003), pp. 2733-2742.

Tréhu, A.M., Bohrmann, G., Torres, M.E., and Colwell, F.S. (Eds.), Proc. ODP, Sci. Results, 204 (2006), pp. 1-19.

von Stackelberg, M., Muller, H.R. “On the Structure of Gas Hydrates.” J. Chem. Phys. 19, 10 (1951), pp. 1319-1320.

Vysniauskas, A., Bishnoi, P.R. “A Kinetic Study of Methane Hydrate Formation.” Chemical Engineering Science 38, 7 (1983) 1061-1072.

Yousif, M.H., “The Kinetics of Hydrate Formation.” SPE 69th Annual Technical Conference and Exhibition, New Orleans (1994): SPE 28479.

Zhong, Y., Rogers, R.E. “Surfactant Effects on Gas Hydrate Formation.” Chemical Engineering Science 55 (2000), pp. 4175-4187.

Vita

Divya Ramaswamy was born in Mumbai, India, in 1987. She graduated with a Bachelors degree in Chemical Engineering from Anna University, Chennai, India, in May 2008 and joined The University of Texas at Austin to pursue Masters in Petroleum Engineering in August 2008.

Email address: divya.r@utexas.edu

This thesis was typed by the author.